GLP-1 receptor agonist treatment improved fasting and postprandial lipidomic profile independently of diabetes and weight loss

Running title: **GLP-1RA effect on lipidomic profile**

Giuseppe Della Pepa MD, PhD[1*], Bárbara G. Patrício PhD [1,2*], Fabrizia Carli PhD[1], Silvia Sabatini PhD[1], Brenno Astiarraga PhD [3,4,5], Ele Ferrannini MD [1,3], Stefania Camastra MD [3], Amalia Gastaldelli PhD [1,2,#]

[1] National Research Council (CNR), Institute of Clinical Physiology (IFC), Pisa, Italy;
[2] Sant'Anna School of Advanced Studies, Pisa, Italy;
[3] University of Pisa, Department of Clinical and Experimental Medicine, Pisa, Italy
[4] Pere Virgili Institute for Health Research (IISPV), Terragona, Spain
[5] CIBER de Diabetes y Enfermedades Metabólicas Asociadas (CIBERDEM)-Instituto de Salud Carlos III (ISCIII), 28029, Madrid, Spain

* Equally contributing authors
Word count abstract: 244
Word count article: 4001
Figures: 5
Supplementary table: 3

[#]Corresponding author:
Amalia Gastaldelli
Institute of Clinical Physiology, CNR
Via Giuseppe Moruzzi 1, 56124 Pisa Italy
E-mail amalia.gastaldelli@cnr.it

Highlights

- Few data are available on the effect of glucagon-like peptide-1 receptor agonists (GLP-1RAs) on lipid metabolism and no information on the postprandial lipidomic profile.

- In non-diabetic adults with severe obesity, 3-month treatment with exenatide improved fasting and postprandial lipidomic profile associated with cardiometabolic risk (CMR) by decreasing saturated species (TAGs, CERs, LPCs) while increasing 7 unsaturated phospholipid species (PC, LPC) with protective effects on CMR compared to control.
    - Exenatide blunted the rise in postprandial triglycerides especially saturated TAGs.
    - Postprandial triglycerides reduction was associated to decreased postprandial FFA clearance, with lower saturated FFA incorporation into newly synthesized lipids (TAGs and CERs).

Abbreviations: Apo: apolipoprotein; BMI: body mass index; CER: ceramides; CMR: cardiometabolic risk; CT: control; CVD: cardiovascular disease; DAG: diacylglycerols; DNL: de novo lipogenesis; DPP-4: dipeptidyl peptidase; EXE; exenatide; FFA: free fatty acid; GIP: gastric inhibitory peptide; GLP-1 RA: glucagon-like peptide-1 receptor agonist; HDL: high-density lipoprotein; LDL: low-density lipoprotein; LPC: lyso-phosphatidylcholines; MASLD: metabolic associated-dysfunction steatotic liver disease; MTT: mixed meal tolerance test; OGTT: oral glucose tolerance test; PC: phosphatidylcholines; PE: phosphatidylethanolamines; SFA: saturated fatty acid; SM: sphingomyelins; TAG: triacylglycerols; AUC: area under the curve; T2D: type 2 diabetes; VLDL: very low-density lipoproteins

Abstract
Treatment with glucagon-like peptide-1 receptor agonists (GLP-1RAs) reduces liver steatosis and cardiometabolic risk (CMR). Only few data are available on lipid metabolism and no information on the postprandial lipidomic profile. Thus, we investigated how exenatide treatment changes lipid metabolism and composition during fasting and after a meal tolerance test (MTT) in adults with severe obesity without diabetes. Thirty individuals (26F/4M, 30-60 years old, BMI>40 kg/m2, HbA1c=5.76%) were assigned (1:1) to diet with exenatide treatment (EXE, n=15, 10 µg twice-daily) or without treatment as control (CT, n=15) for 3 months. Fasting and postprandial lipidomic profile (by LC/MS-QTOF) and fatty acid metabolism (following a 6-hour MTT/tracer study) and composition (by GC/MS) were evaluated before and after treatment. Both groups had slight weight loss (EXE: -5.5% vs CT: -1.9%, p=0.052). During fasting, exenatide, compared to CT, reduced some ceramides (CER) and lysophosphocholines (LPC) previously associated with CMR, while relatively increasing unsaturated phospholipid species (PC, LPC) with protective effects on CMR, although concentrations of total lipid species were unchanged. During MTT, both groups suppressed lipolysis equally to baseline, but EXE exenatide significantly lowered free fatty acid clearance and postprandial t
riacyclglycerols (TAG) concentrations, particularly saturated TAGs with 44-54 carbons. Exenatide also reduced some postprandial CERs, PCs, LPCs previously linked to cardiometabolic risk. These changes in lipidomic profile remained statistically significant after adjusting for weight loss. Exenatide improved fasting and postprandial lipidomic profile associated with CMR mainly by reducing saturated postprandial TAGs and CERs, independently of weight loss and diabetes.
Keywords: GLP-1 receptor agonist; obesity; lipidomic; postprandial lipemia; free fatty acids; phospholipids; ceramides.

Graphical abstract

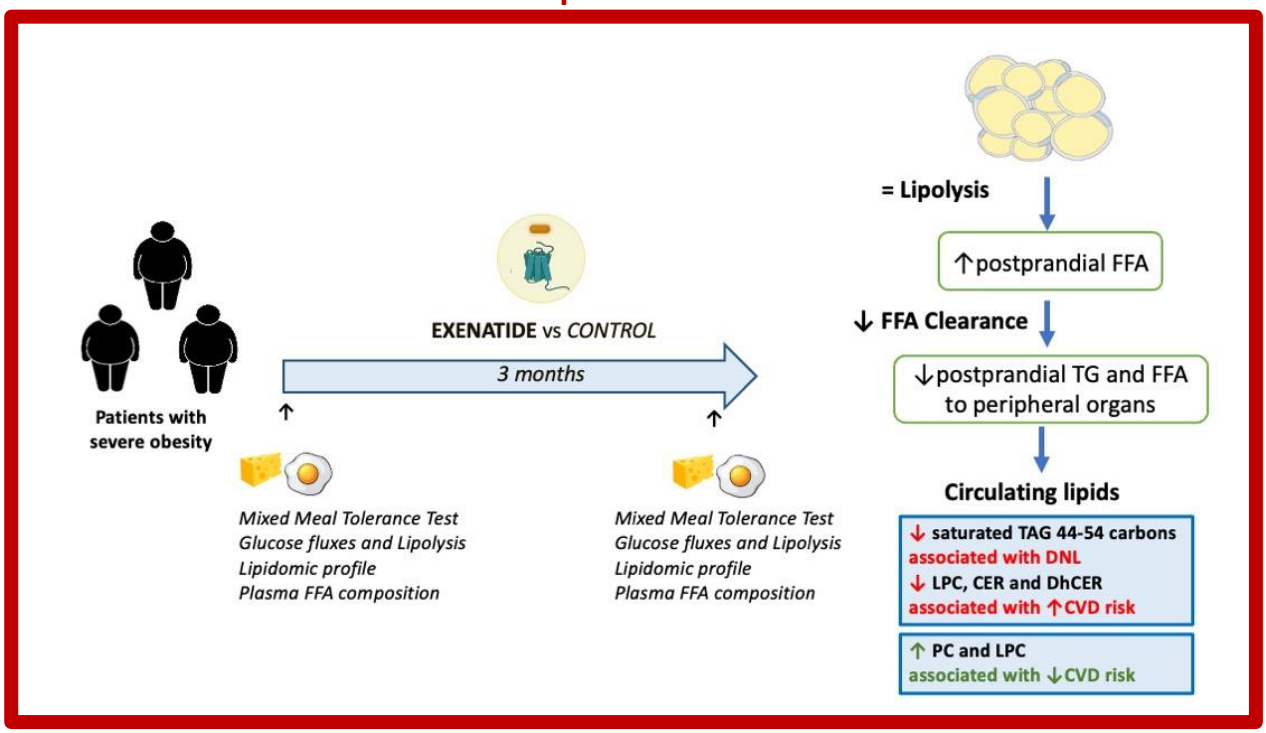

.

Introduction

It is well established that treatment with glucagon like peptide-1 receptor agonists (GLP-1 RAs) improves glucose control, slows down gut motility, and promotes satiety and weight loss; a beneficial impact on steatotic liver disease (SLD), nephropathy and cardiovascular morbidity and/or mortality has been consistently reported (1; 2). It is likely that some of these benefits are due to changes in lipid profile, particularly lipids secreted by the liver as triglycerides (TAGs) and ceramides (CERs) (2). However, the reduction of cholesterol and TAG concentrations by GLP-1RA is modest (1). Only few studies that have investigated the effect of GLP-1/GLP-1RA on postprandial lipid metabolism and postprandial lipemia focusing on changes in lipoprotein metabolism after treatment with DPP-4 inhibitors (3), liraglutide (4; 5), lixisenatide (6), or semaglutide in subjects with obesity (7). A positive effect of GLP-1RA was observed on postprandial lipoprotein metabolism, showing a reduction in very low-density lipoproteins (VLDL) assembly and secretion (2; 4; 5) and chylomicron (4-6).

It is likely that the reduction in TAGs is mediated via changes (e.g., reduction) in circulating fatty acids. Hepatic VLDL is constituted mainly from TAG-containing fatty acids derived from adipose tissue lipolysis (around 59%) (8). The LEAN study showed that 48-weeks liraglutide treatment not only decreased liver fat, but also free fatty acid (FFA) concentrations, lipolysis and hepatic *de novo* lipogenesis (DNL) (9; 10). Exenatide injection before an oral glucose tolerance test (OGTT) showed an improvement in the adipo-IR index, indicating less FFA release and/or increased intracellular re-esterification compared to placebo (11). However, GLP-1RA has no direct effect on the suppression of peripheral lipolysis as GLP-1 infusion during a pancreatic clamp did not alter lipolysis or FFA concentrations (12).

Besides lipoproteins and TAGs, which are the most studied lipids, other lipid species are markers of lipotoxicity and insulin resistance, like CERs, diacylglycerols (DAGs) and some phosphocholines (PCs) (13), also associated with cardiometabolic risk (CMR) (14). CERs are also associated with the risk of incident MACE in apparently healthy individuals and allowed a better stratification of subjects at risk compared to LDL cholesterol (15; 16). However, data on changes in the lipidomic profile after GLP-1RA treatments are lacking and the few studies available considered only the fasting state (17-20). In fasting state, treatment with GLP-1RAs reduced CERs, sphingomyelins (SMs), cholesterol esters (CEs), lysophosphatidylcolines (LPCs) and PCs (17-20). All these studies were conducted in subjects with type 2 diabetes (T2D), and the improvement could be mediated by changes in glycemic control and significant weight loss. Moreover, although GLP-1 is a postprandial hormone, there are no studies about the effect of GLP-1RA treatment on lipidomic profile in postprandial state, particularly for lipids associated with risk of cardiovascular events like CERs.

Thus, the aim was to evaluate the effects of 3-month treatment with exenatide on the fasting and postprandial lipidomic profile compared with no-treatment control in subjects with severe obesity without T2D.

Research Design and Methods

Participants and study design

The study details were previously published (21). Briefly, thirty study participants with severe obesity of both genders (26F/4M), BMI ≥40 kg/m^2, without T2D (mean HbA1c=5.76%), waitlisted for bariatric surgery (**Supplementary Table 1**) were unblinded assigned (1:1 ratio) to the maximum dose of exenatide (10µg twice daily, EXE, n=15) or no-treatment (CT, n=15) for 3-months in combination with diet (caloric intake as the estimated resting metabolic rate). Subjects were asked to maintain the assigned diet, habitual physical activity, and no engagement in a structured exercise program was allowed. Control visits were carried out 30 and 60 days with laboratory measurements and monitoring of treatment compliance.

A mixed meal tolerance test (MTT) was carried out at baseline and end of treatment. Arterialized blood samples were taken before and for 6 hours after the meal (i.e., -120 -15, 0. 15, 30, 45, 60, 90, 120, 150, 180, 240, 300 and 360 min) for FFAs, TAGs and tracer enrichment to evaluate lipid fluxes and insulin resistance indexes (**Supplementary)**. Apolipoprotein concentrations and lipidomic analyses were conducted at 0, 180min and 360min.

The study protocol – performed per the Declaration of Helsinki – was approved by the Pisa Institutional Ethics Committee, and all participants provided written informed consent to use their clinical and laboratory data and to be included in the study.

Lipids and lipidomic profile

Total triglycerides (Beckman Instruments, Fullerton, California) and FFA (Fujifilm WAKO Chemicals, Neuss, Germany) concentrations were assayed by standard spectrophotometric methods, apolipoproteins by immunoturbidimetric method

(Apo-A1 and Apo-B, Randox Laboratories, Crumlin, UK).

Plasma lipidomic profile (TAG, DAG, CER, SM, PC, LPC, PE) was quantified with internal standards by liquid chromatography/mass spectrometry (LC-1290 /MS-Q-TOF-6545, Agilent Technology, Santa Clara, CA) and FFA composition by gas chromatography-mass spectrometry (GC7890-MS5975, Agilent Technology) (22), details in **Supplementary**.

Calculations and statistical analysis

Peripheral FFA uptake was calculated as:

$Rd\_FFA_{\mu mol/min}(t) = Lipolysis(t) - dFFA_{\mu mol/ml}(t)/dt \times Vol(ml/kg) \times BW(kg)$

where lipolysis was quantified as (3 x Ra_glycerol) measured by $^2H_5$-glycerol infusion, $dFFA_{\mu mol/ml}(t)/dt = [FFA_{\mu mol/ml}(t) - FFA_{\mu mol/ml}(t_1)]/(t-t_1)$ and $Vol(ml/kg) = 70/\sqrt{(BMI/22)}$ is the volume of distribution for subjects with severe obesity (23)

$FFA_{l/ml}$ clearance(t) = $Rd\_FFA_{\mu mol/ml}$ (t) / $FFA_{\mu mol/l}$ (t)

VLDL concentrations were calculated as (24):

VLDL = triglycerides/8.59 + triglycerides x Non-HDL/2250 – triglycerides^2/16500

Data are presented as mean ± standard deviation (SD) for tables or mean ± standard error of the mean (SEM) for figures, unless stated otherwise. The area under the curve (AUC) was calculated using the trapezoidal rule from 0-180 min and 180-360 min to account for the effect of exenatide in delaying the gastric emptying.

Paired *t-test* and Wilcoxon Signed Rank test were used for variables with normal and non-normal distribution respectively, Kruskal Wallis test and generalized linear model (GLM) multivariable analysis (SPSS 26.0, IBM, Armonk, NY, USA) were used to evaluate differences between groups calculated as changes (3-month *minus* baseline values) with changes in weight (kg) added as covariates to disentangle the effect on the lipidomic profile from weight loss.

Spearman correlation and GLM adjusted for treatment and weight changes were used to assess the effect of changes in insulin resistance indexes, triglycerides, glucose and hormones on changes in FFA clearance and concentrations. Statistical significance was set at $p < 0.05$ (two tails). Figures were done using R software version 4.2.1, package.

Data and Resource Availability

Data sets and resources are available upon request.

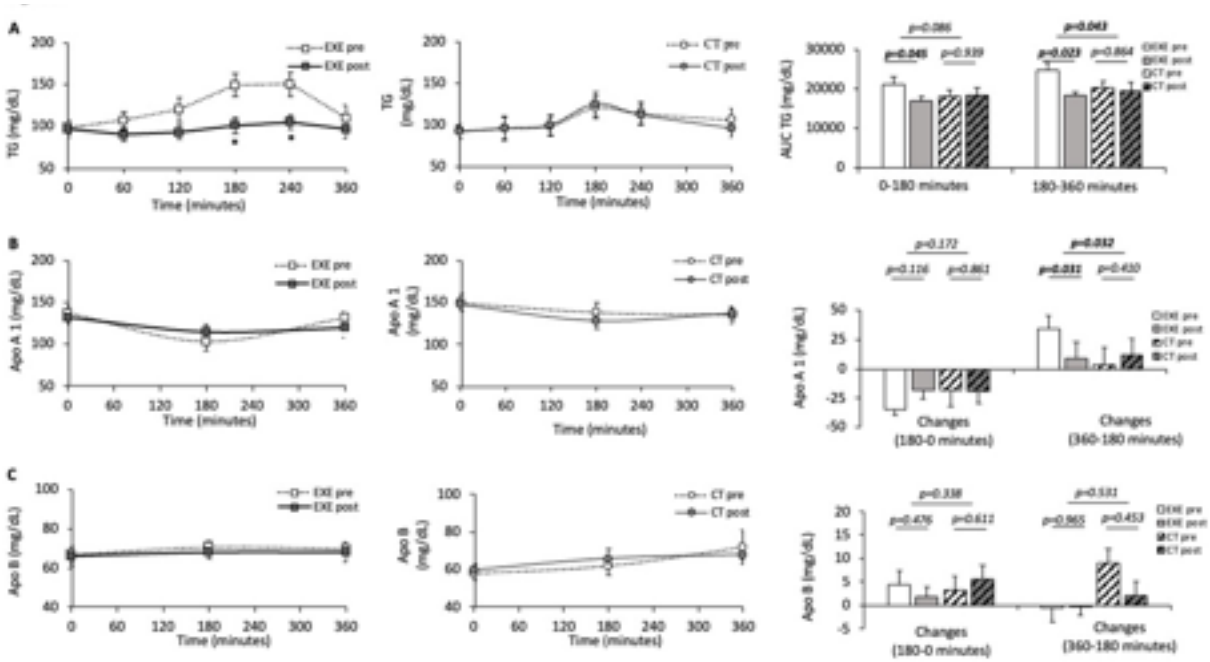

Figure 1. Postprandial levels and area under the curve or changes for triglyceride **(A)**, apolipoprotein A1 **(B)** and apolipoprotein B **(C)** during the standard meal in Exenatide and control before and after 3 months of treatment. Within-group comparisons were performed by paired-samples t-test; between-group comparisons of treatment (EXE and CT) induced changes (3-month minus baseline values) were performed by ANCOVA general linear model. EXE: exenatide; CT: control; TG: triglycerides; APO: apolipoprotein.

Results

Effect of exenatide on clinical parameters

These two groups with severe obesity (BMI>40 kg/m^2, HbA1c=5.76%) had similar baseline anthropometric parameters, fasting and postprandial concentrations of glucose, insulin, GLP-1, GIP, and glucagon (**Supplementary Table 1**).

After 3 months, weight (-6.7±5.0 kg for EXE vs -2.3±6.0 kg for CT, p=0.039) and BMI (-2.5±1.7 for EXE vs -0.9±2.3 for CT, p=0.043) were significantly decreased in EXE compared with CT, but percent weight reduction was not statistically different (-5.5% for EXE vs -1.9% for CT, p=0.052). Most of the weight loss was due to a decrease in fat mass in the EXE group, but this change did not reach statistical significance vs CT (p=0.097).

Fasting insulin was significantly decreased after EXE compared with CT, while fasting glucose, GLP-1, GIP, and glucagon concentrations did not change in both groups.

Postprandial glucose, insulin, glucagon, GLP-1, and GIP concentrations were significantly lowered by EXE during the first 3 hours after the meal ingestion, particularly from 60 to 180min. Moreover, whole-body insulin sensitivity (OGIS index) was significantly improved in the EXE-group compared with baseline and the CT-group (**Supplementary Table 1**).

Effect of exenatide on fasting and postprandial TG and FFA concentrations and fluxes

Fasting values of total TAGs, Apo-A1, Apo-B, and FFA were similar and within the normal ranges before treatment (**Supplementary Table 1**) and did not change after 3-months in either group (**Figure 1-2**). In contrast, the increase in postprandial TAG concentration was significantly decreased (-26%) in the later part of the curve ($AUC_{180\text{-}360min}$) in the EXE-group while it did not change in the CT-group (**Figure 1A**). No change was observed in postprandial Apo-A1 and Apo-B concentrations compared to the baseline study or CT (**Figure 1B, 1C**). Fasting FFA concentrations were also not modified by EXE treatment.

Before treatment, postprandial insulin suppressed FFA concentrations during the first 180 min after the meal, returning to fasting values after 360 min in both groups. CT-group did not change the FFA profile compared to pre-study, while EXE-group had higher FFA concentrations at 120, 150, and 180 min and significantly lower at 15 and 360 min compared to pre-study (p<0.05 for all); $AUC_{0\text{-}180min}$ was significantly higher in EXE than CT-group (**Figure 2A, 2B**)

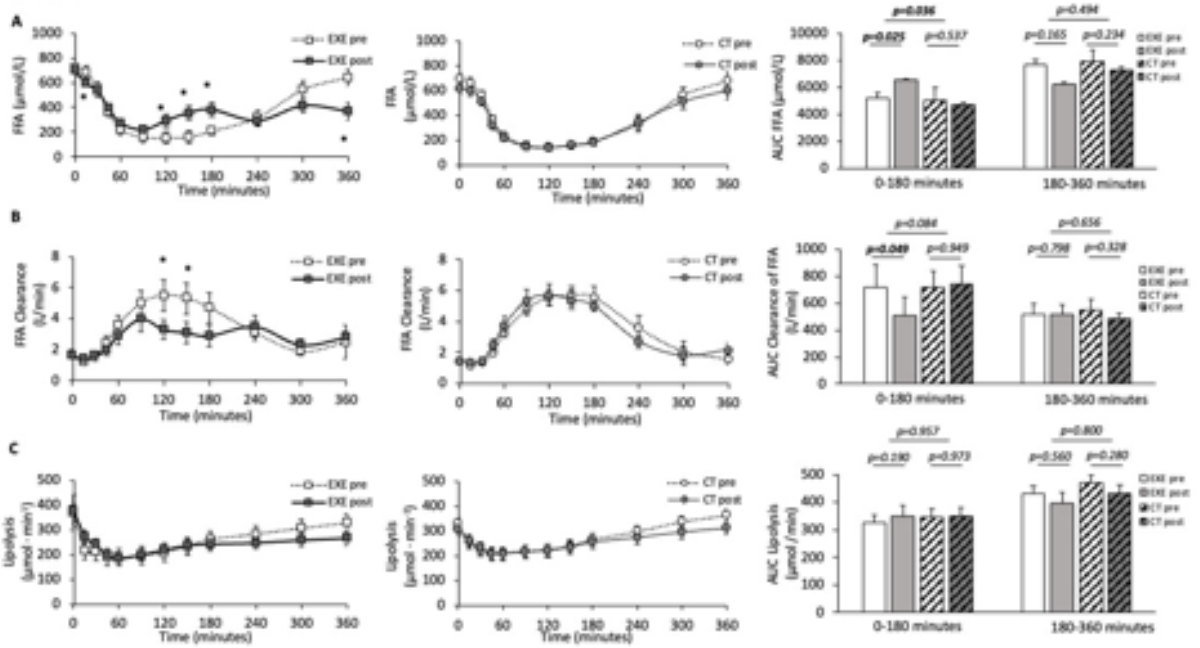

Figure 2. Postprandial levels and area under the curve for free fatty acids **(A)**, clearance of free fatty acids **(B)** and lipolysis **(C)** during the standard meal in exenatide and control before and after 3 months of treatment. Within-group comparisons were performed by paired-samples t-test; between-group comparisons of treatment (EXE and CT) induced changes (3-month minus baseline values) were performed by ANCOVA general linear model. EXE: exenatide; CT: control; FFA: free fatty acids

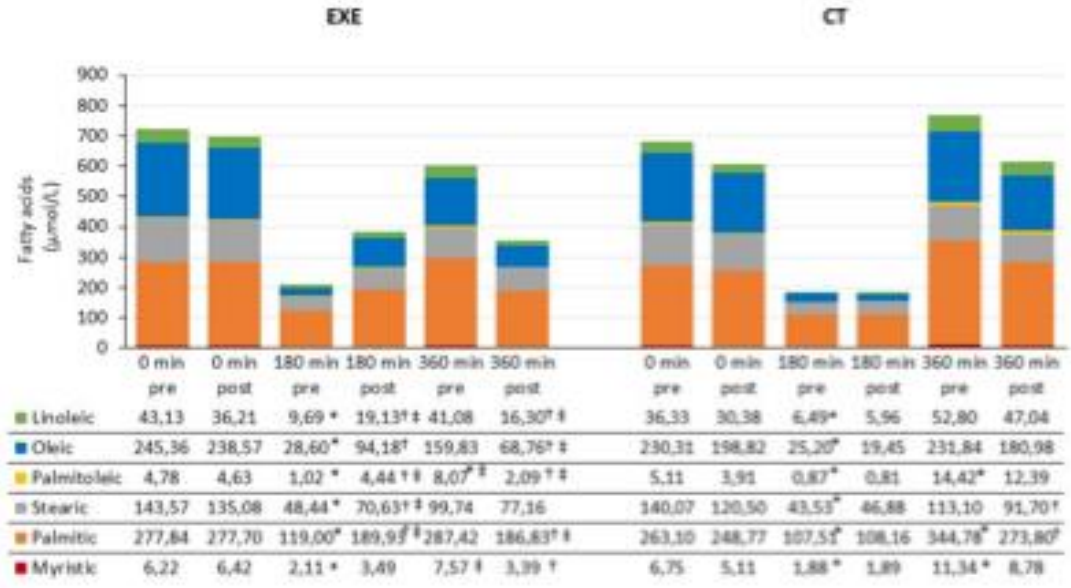

Figure 3. Postprandial levels of single free fatty acids during the standard meal in Exenatide and control before and after 3 months of treatment. *p<0.05 vs pre 0 min, †p<0.05 vs pre same time, ‡p<0.05 EXE vs CT same time. Within-group comparisons were performed by paired-samples t-test; between-group comparisons of treatment (EXE and CT) induced changes (3-month minus baseline values) were performed by ANCOVA general linear model. EXE: exenatide; CT: control; FFA: free fatty acids.

The mechanisms responsible for higher postprandial FFA concentrations in EXE were investigated by looking first at adipose tissue lipolysis, measured as rate of glycerol release by tracer infusion, and FFA clearance, an index of peripheral FFA metabolism. Lipolysis did not change with EXE treatment, nor it was different between groups (**Figure 2C**). On the other hand, the postprandial clearance rate of FFA was reduced by EXE in the first part of the curve ($AUC_{0\text{-}180min}$) compared with the CT-group, with a trend in differences between groups (p=0.095), (**Figure 2B**). In particular, EXE significantly lowered postprandial FFA clearance at 120 and 150 min (p<0.05 for all) compared with rates before treatment and vs the CT-group (**Figure 2B**). The changes in FFA clearance rate in the first 3 hours of the MTT were found correlated with the improvement in HOMA-IR and OGIS, glucose and insulin profile and remained significant after adjusting for treatment and changes in weight (**Supplementary Table 3**).

Effect of exenatide on fasting and postprandial lipidomic profile and individual lipid species

Lipidomic profile, i.e., FFA, TAG, phospholipids, like PC and LPC, PE and LPE, and CER composition, was measured during fasting and postprandial state to investigate whether EXE treatment induced significant changes.

Fasting FFA composition, which reflects adipose tissue composition (25), was similar in the two groups at baseline and at follow-up (about 60% saturated fatty acids (SFA) and 40% unsaturated fatty acid (UFA)) (**Figure 3**).

In contrast, postprandial FFA composition showed several differences: before treatment, the maximal reduction in FFA concentrations was observed at 180 min due to both low lipolysis and high FFA clearance rates (**Figure 2**). However, SFA constitute the majority of circulating FFA at 180min (more than 80%) in both groups (**Figure 3**), indicating that in postprandial state more UFA than SFA are taken up by peripheral tissues to be esterified as TAGs or used for the synthesis of other lipids. Postprandial FFA concentrations in the EXE-group were higher between 120 and 180 min compared to baseline study due to lower clearance rates, since lipolysis rate was similar to baseline profile, and did not raise back to fasting concentrations (**Figure 2**); also, the composition of these FFA was different compared to baseline and CT containing about 70% of SFA and 30% of UFA (**Figure 3**).

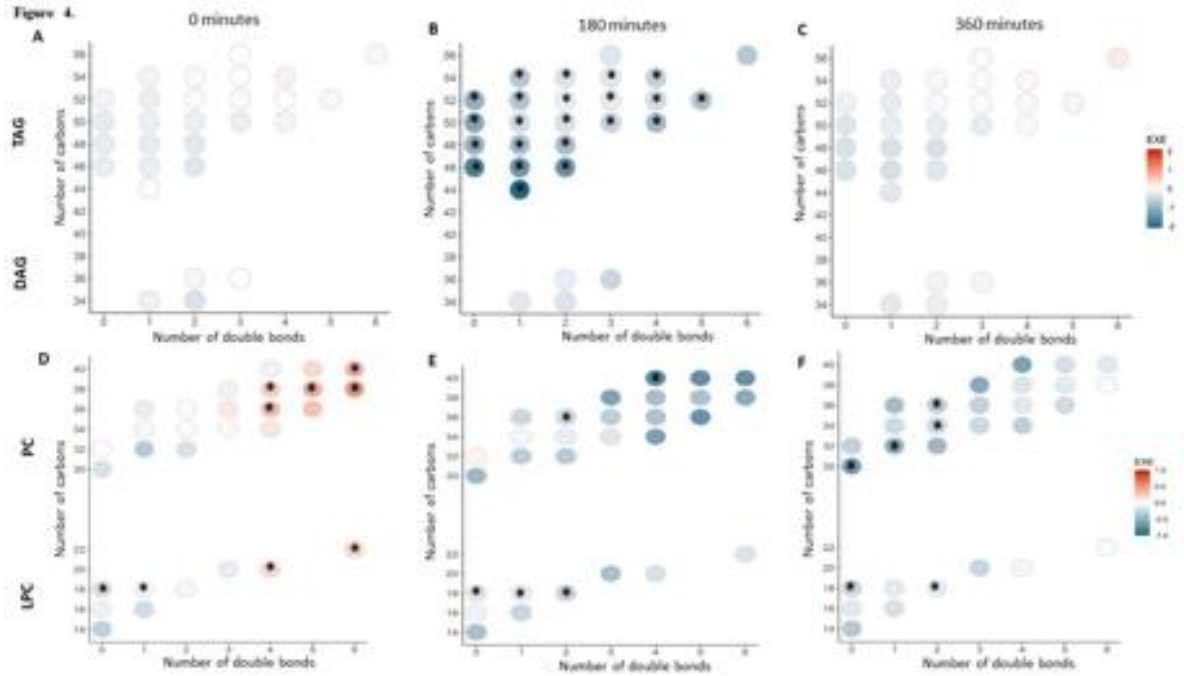

Figure 4. Changes (3 months *minus* baseline values) after the standard meal in the group treated with Exenatide in triacylglycerols (TAG) and diacylglycerols (DAG) at fasting (0 minutes) (**Panel A)**, 180 minutes (**Panel B)** and 360 minutes **(Panel C),** and in phosphatidylcholine (PC) and lysophosphatidylcholine (LPC) at fasting (0 minutes) (**Panel D),** 180 minutes (**Panel E)** and 360 minutes **(Panel F).** Blue color indicates reduction compared to pre-study; color red indicate increase compared to pre-study at each time points. *p<0.05 vs CT. EXE: exenatide; CT: control; TAG: triacylglycerol; DAG: diacylglycerol; PC: phosphatidylcholine; LPC: lysophosphatidylcholine.

Interestingly, the changes in palmitate concentrations at 180min due to a reduced clearance were negatively associated with the decrease in TAGs in the first 3 hours (**Supplementary Table 3**). This result explains, at least in part, the decrease in postprandial TAGs, especially in saturated TAGs (**Figure 4B**), which have been shown to be synthesized mainly by circulating FFA (8).

At fasting, the composition of TAGs, DAGs, CERs, SMs, PCs and LPCs was comparable in the two groups before treatment (**Supplementary Table 2**). After 3 months, there was no change in the fasting state concentration of the sum of TAG, DAG, SM PC, LPC, CER species in both groups **(Supplementary Table 1**), but there was an increase in the EXE-group in some phospholipids previously found to be associated with a protective effect on CMR, i.e. PC aa(36:4), PC aa(38:4), PC aa(38:5), PC aa(38:6), PC aa(40:6), and LPC(20:4), and a decrease in some LPCs associated with progression of atherosclerotic plaque, i.e., LPC(18:0), LPC(18:1) compared to baseline and CT (**Figure 4D, Supplementary Table 2**). Furthermore, in the EXE-group, we observed a significant reduction in fasting CER(18:1/14:0), CER(18:1/20:0), and CER(18:1/22:0), also previously associated with incident cardiovascular disease (CVD) **(Figure 5A).**

During the first 180 min of the MTT, EXE significantly reduced several TAGs, but not DAGs, compared to CT and to baseline, particularly saturated TAGs containing 44-54 carbons (including those derived mainly through DNL (26)) due to a decreased FFA clearance and incorporation of SFA, consistent with the postprandial FFA profile **(Figure 4B),** while no change was observed at 360 min or in CT (**Figure 4C**). A similar profile was observed also in PC and LPC profile **(Figure 4E, 4F**). CERs were slightly decreased in the EXE-group during fasting while there was a trend to be increased in the CT-group, but it was in the later postprandial phase state (360 min after the meal) that were observed the major changes, i.e., a significant reduction in EXE (and an increase in CT) of CER(18:0/20:0), CER(18:0/22:0), CER(18:0/24:0), CER(18:0/26:0), CER(18:1/14:0), CER(18:1/20:0), CER(18:1/22:0), CER(18:1/24:0), and CER(18:1/26:0) **(Figure 5C)**.

The effects of EXE compared with CT on fasting and postprandial lipidomic profile changes remained statistically significant after adjusting for weight changes observed at the end of treatment (**Supplementary table 2**).

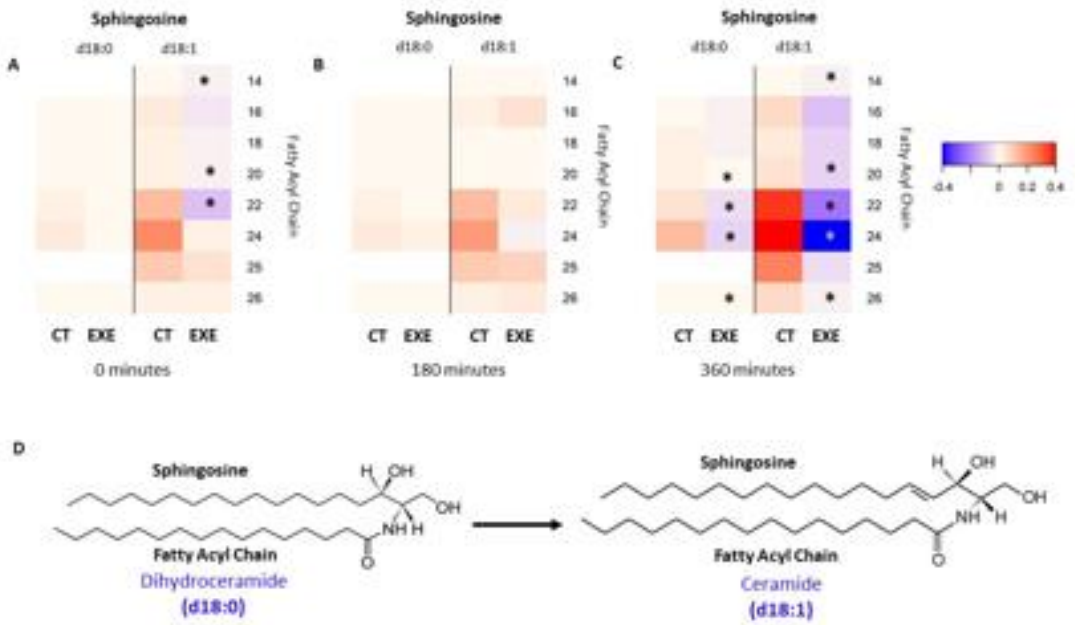

Figure 5. Heatmap of Delta (post - pre) of ceramide concentrations in the group treated with Exenatide compared with the control groups at fasting (**Panel A**), 180 minutes (**Panel B**) and 360 minutes (**Panel C**) after the standard meal. d18:0 indicates dihydroceramides, d18:1 indicates ceramide. **Panel D:** Dihydroceramide and ceramide structures. Ceramides are composed of a sphingosine (obtained from the condensation of serine and palmitoyl-coA) and a fatty acid. Blue color indicates reduction compared to pre-study; color red indicate increase compared to pre-study at each time points. *p<0.05 vs CT. EXE: exenatide; CT: control; CER: ceramide.

Discussion

GLP-1RA are widely used for their significant effects on glycemic control and weight loss (1; 27), but less is known about their effects on postprandial changes in lipid turnover and lipidomic profile. In this study we analyzed the effect of exenatide BID, a GLP-1RA with a short half-life (about 2-4 hours in humans) and duration of action, in subjects with severe obesity without diabetes. Compared to the newer GLP-1 RAs (i.e. liraglutide, dulaglutide and semaglutide) that have long pharmacokinetics (27), the concentrations of exenatide BID peaks within 2 hours after administration but after 7-8 hours its serum concentration is very low (28), thus with a time of action closer to that of endogenous GLP-1 that peaks in the postprandial state and then rapidly decreases to fasting levels.

Our previous study (21) showed that exenatide improved fasting insulin sensitivity in liver, muscle and adipose tissue, and in postprandial state delayed oral glucose appearance in the circulation, thus lowering postprandial glycaemia, but also decreased glucagon response without changes in β-cell function.

Although exenatide did not change the rate of lipolysis, this post-hoc analysis showed that exenatide had significant fasting and postprandial effects on lipidomic profile and fatty acid clearance in postprandial state in particular: 1) exenatide, compared to control, improved fasting and postprandial lipotoxicity by decreasing some fasting and postprandial LPCs and CERs associated to CMR and increasing fasting PCs associated with a protective effect on CMR; 2) exenatide reduced the postprandial rise in TAGs that included less saturated TAGs containing 44-54 carbons: this was mainly associated with lower SFA incorporation of into newly synthesized lipids due to significant reduction in postprandial FFA clearance, while not changing rate of lipolysis; and lower concentration of TAGs synthesized through DNL (i.e. containing palmitic acid) and previously associated with risk of diabetes (29).

Changes in fasting and postprandial lipid profiles remained significant after adjustment for weight loss and this is important given that weight loss significantly changes the lipidomic profile (30). Moreover, as the subjects did not have diabetes, and neither their fasting glucose concentrations nor glycated haemoglobin (slightly above the pre-diabetes threshold) changed at the end of the intervention, glycaemic control also did not play a role.

To the best of our knowledge, this is the first study investigating the effects of GLP-1RA on lipid composition in response to MTT and in subjects without T2D, i.e., excluding the possible involvement of T2D in alteration in lipid metabolism, which is common in these subjects (31). In our study, the reduction in circulating palmitic acid at 180min

correlated with the improvement in OGIS and HOMA-IR and the association remained significant (p=0.002) also after adjusting for treatment and weight loss (**Supplementary Table 3**).

Previous studies showed that GLP-1RA treatment in subjects with T2D induces a significant, although modest, decrease in total cholesterol, HDL and LDL cholesterol or fasting TAGs (1), explaining only in part the GLP-1RA beneficial effects on decreasing CMR and cardiovascular events. However, other lipid species are associated with a worse cardiometabolic profile, e.g., lipids rich in SFA, as sphingolipids like SM and CER or phospholipids, like PC, PE and LPC (14; 16; 32-34). These lipotoxic compounds are associated with the development of insulin resistance and organ damage (13; 29; 35) increasing CMR (36; 37).

We found that exenatide decreased several lipids rich in SFA, like CER and LPC previously associated with MASLD (14; 35) and CMR (20; 33). During fasting, a significant reduction was observed in CER(18:1/14:0), CER(18:1/20:0), and CER(18:1/22:0), which are toxic species associated with MASLD (14; 35) and CMR (16; 20; 33); no change was observed in fasting dihydroceramides. In contrast exenatide induced a significant increase of lipids that contains mainly UFA, i.e., PC aa(36:4), PC aa(38:4), PC aa(38:5), PC aa(38:6), PC aa(40:6), and LPC(20:4), found to be associated with a protective effect on CMR (32; 34).

These results are in line with previous reports. Liraglutide significantly decreased fasting CER, PC, LPC, and PE in adult individuals with obesity and T2D after 18 weeks of treatment (18). Similarly, exenatide treatment for 3 months significantly decreased fasting SM, LPC, and PE in adult individuals with obesity and T2D (19). Similar results especially on CERs were shown using liraglutide for 6 months vs placebo (17) or healthy controls (20).

Exenatide had no effect on fasting TAGs, but reduced postprandial TAG concentrations, confirming previous reports in subjects with T2D treated with acting (4-6; 38-40) or long acting GLP-1RAs (7; 41). These were TAGs rich in SFA, previously associated with high risk of diabetes (29) and CVD (42). In this study total apolipoprotein B (i.e., Apo-B-48 plus Apo-B-100) concentration did not change during the MTT or in response to treatment, excluding that the changes in TAGs were due to decreased synthesis of chylomicrons or VLDL.

Interestingly, the baseline analysis shows that postprandial FFA are richer in SFA compared to the fasting state (**Figure 3**), suggesting that in general more UFA are taken up by peripheral tissues to be esterified as TAGs or used for the synthesis of other lipids in the postprandial state, i.e., when triglyceride assembly and secretion is increased. This is consistent with data on the composition serum TAGs, which show high content of UFA (oleate 37.7%, linoleate 15%, palmitoleate 5.1%) vs SFA (palmitate 29.5%, stearic 4.5% and myristic acid 3.3%) (43). VLDL triglycerides are composed mainly by FFA derived from adipose tissue lipolysis (59%), and only 15% from dietary fatty acids (8). These and our results indicate that for TAG assembly the liver preferentially uses UFA derived from adipose tissue, whereas TAG-SFA are from DNL, whose main product is palmitate and contributes to approximately 26% of the fatty acids in circulating TAGs (8).

Exenatide was associated with less suppressed FFA during postprandial state, in agreement with previous studies (39). Exenatide did not change peripheral lipolysis that was suppressed similarly to baseline, confirming that GLP-1 does not act on adipose tissue (12). Interestingly, exenatide blunted the increase in FFA clearance in the first 180min, favoring the reduction in FFA-SFA, thus affecting both FFA concentration and composition (**Figure 2 and 3**). This effect may have a beneficial impact on CMR, considering that higher stearic and palmitic acid concentrations at 2h-OGTT were independently associated with increased risk of incident T2D in a large Chinese cohort followed for 7 years (44). Again, a strong negative correlation was found between palmitate clearance rate and whole-body and muscle insulin sensitivity in obese individuals (45).

Although the reduction in postprandial TAGs was modest, this was accompanied by a large modification in TAG composition, with less saturated long-chain fatty acids at 180 min especially those derived by DNL (26) like TAG(46:0), TAG(46:1), TAG(46:2), TAG(48:0), TAG(48:1), TAG(48:2) and TAG(50:0) (**Figure 4)**. Of note, we cannot exclude a possible role of glucagon on TAG changes, by promoting hepatic fatty acid β-oxidation while suppressing DNL. Vega et al. (46) reported a marked reduction of TAGs and DAGs following glucagon infusion in healthy individuals with overweight/obesity, but in our study no correlation was observed between changes in fasting/postprandial glucagon and TAGs. The increase at 180 min in the TAG's saturated component was then suppressed at the end of the postprandial phase, 360 min (**Figure 2** and **3**), thereby paralleling the time-course of insulin concentrations (21). The mechanism by which exenatide decreases FFA clearance is unknown, but it might also be related to hepatic fatty acid

transport, since in mice it has been shown a decrease in CD36, together with an improvement in lipidomic profile and insulin resistance, after treatment with exenatide (47). The reduction in FFA clearance could be related also to lower insulin concentrations in postprandial state (**Supplementary Table 3**).

During the first 3 hours after the meal, exenatide reduced also several PCs and also some LPCs, particularly LPC(18:0), LPC(18:1), LPC(18:2) associated with progression of atherosclerotic plaque (48). This is of particular interest since alterations in fasting lipidomic profile (i.e., SFA, phospholipids, like PC and LPC, PE and LPE, and CER) have been associated with increased risk of CVD and metabolic dysfunction including MASLD (14; 16; 42; 49). In the later phase after the meal, 360 min, both dihydroceramides and CERs previously reported to be associated with cardiovascular risk factors and MACE (15; 16) were further reduced (**Figure 5**).

The main changes in lipidomic profile occurred mainly in the postprandial state, whereas we observed little change in fasting lipid species, probably because the fasting lipid profile was not particularly altered in these subjects who did not have comorbidities.

Our study has several strengths and novelties. We investigated the effect of exenatide on the postprandial lipidomic profile, which has never been investigated before, including a wide range of lipid species. These results were resistant to the adjustment by weight changes as a covariate in the statistical model, suggesting that weight loss is not the major player in the observed findings. Exenatide is less potent than the current GLP-1Ras (i.e., liraglutide, dulaglutide and semaglutide), so we can expect that other GLP-1RAs and/or longer treatment may result in further changes. Secondly, as this study was performed in subjects without T2D, these results are also independent of the improvement in glycemic control and may provide new insights into the mechanisms behind the beneficial effects of GLP-1RAs on cardiometabolic diseases.

Finally, the changes in the comprehensive lipids panel (fasting/postprandial lipidomic profile) in the context of changes in insulin sensitivity, glucose and lipid fluxes, measured using stable isotope tracers and mathematical modelling, add further value to the study.

The study has some limitations. The group had a small sample size, consisted of individuals with severe obesity, mainly females, but otherwise healthy, limiting the generalizability of the results. The balanced composition of the MTT, with a 31% fat content, which limits an excessive postprandial lipemic response. A 3-month intervention cannot be considered a true long-term experiment, although it is certainly sufficient to induce changes in most of the newly synthesized lipids, but not in fasting FFA composition. Although the subjects were regularly reminded of their diet during monthly control visits, the habitual dietary composition may have differed between the two groups. The model used to estimate FFA clearance has also some limitations: FFA-Ra was calculated assuming the FFA-to-Ra_Glycerol ratio constant, which may overestimate FFA clearance, especially in postprandial state when the FFA-to- Ra_Glycerol ratio might be lower due to the higher insulin suppression of FFA-Ra than Ra_Glycerol. However, since EXE treatment did not change Ra_Glycerol, as with infusion of GLP-1 (12), we can speculate that the different postprandial FFA concentrations and composition in the EXE-group were due to lower and selective postprandial FFA clearance. However, treatment with long acting single or dual GLP-1RAs may have greater effects on changes in lipidomic profile in individuals with higher CMR, who generally have a worse lipidomic profile (i.e., subjects with multiple cardiovascular risk factors, T2D or CVD) (22; 50).

In conclusion, 3-month exenatide treatment had a beneficial effect on both fasting and postprandial lipidomic profile blunting the rise in postprandial triglycerides, reducing FFA clearance and the concentrations of circulating saturated lipids, like TAGs, CERs and LPCs associated with CMR. Our results expand the knowledge about the pleiotropic effects of GLP-1RA on postprandial CMR factors independent of glycemic control and after accounting for weight loss.

Acknowledgments

We are grateful to the subjects who volunteered for these intense investigations for their generous collaboration and to Demetrio Ciociaro for his support in the laboratory analyses.

Funding: The initial part of this study was supported by an investigator-initiated unrestricted research grant from Amylin Pharmaceuticals, Bristol-Myers Squibb and AstraZeneca who also provided the drug for this study. B.P. obtained Horizon 2020 FOIE GRAS A.G. acknowledges the financial support from the European Union's Horizon 2020 Research and Innovation Programme under the Marie Skłodowska-Curie for the project "FOIE GRAS: Bioenergetic Remodeling in the Pathophysiology and Treatment of Non-Alcoholic Fatty Liver Disease" under grant agreement No. 722619; European

Union's Horizon Europe Research and Innovation Programme for the project "PAS GRAS: De-risking metabolic, environmental and behavioral determinants of obesity in children, adolescents and young adults" under grant agreement No. 101080329; and Horizon 2020 Research and Innovation Programme for the project "Stratification of Obesity Phenotypes to Optimize Future Obesity Therapy" (SOPHIA). SOPHIA has received funding from the Innovative Medicines Initiative 2 Joint Undertaking under grant agreement No. 875534. This Joint Undertaking received support from the European Union's Horizon 2020 research and innovation program, EFPIA, T1D Exchange, JDRF, and Obesity Action Coalition. The communication reflects the authors view. Neither IMI nor the European Union, EFPIA, or any Associated Partners are responsible for any use that may be made of the information contained herein. B.P. was recipient of an Early-Stage Researcher grant under the H2020 FOIE GRAS project.

Duality of Interest

E.F. has served on the Advisory Board of Boehringer Ingelheim/Lilly&Co., Lexicon, Oramed, and Servier; has received research grants from Boehringer Ingelheim/Lilly&Co and Janssen, and speaker fees from Sanofi, Boehringer Ingelheim/Lilly&Co. and MSD. A.G. has served as a consultant for: Boehringer Ingelheim, Eli Lilly and Company, Metadeq Diagnostics and Fractyl Health; has participated in advisory boards for: Boehringer Ingelheim, Merck Sharp & Dohme, Novo Nordisk, Metadeq Diagnostics and Pfizer; and has received speaker's honorarium and other fees from: Eli Lilly and Company, Merck Sharp & Dohme, Novo Nordisk, and Pfizer. The other authors have no conflict of interest to declare regarding this manuscript.

Author contributions

G.D.P. and B.G.P. analyzed the data and wrote the original draft. B.G.P., F.C., B.A., and S.S. performed lipidomic analysis and acquired the data. S.S. analyzed the data. A.G., S.C., and E.F. performed conception and design of the study, interpretation, and critical revision of the manuscript. A.G. is the guarantor of this work and, as such, had full access to all the data in the study and takes responsibility for the integrity of the data and the accuracy of the data analysis.

Reference

1. Nauck MA, Meier JJ, Cavender MA, Abd El Aziz M, Drucker DJ: Cardiovascular Actions and Clinical Outcomes With Glucagon-Like Peptide-1 Receptor Agonists and Dipeptidyl Peptidase-4 Inhibitors. Circulation. 2017;136:849-870

2. Svegliati-Baroni G, Patricio B, Lioci G, Macedo MP, Gastaldelli A: Gut-Pancreas-Liver Axis as a Target for Treatment of NAFLD/NASH. Int J Mol Sci. 2020;21

3. Matikainen N, Manttari S, Schweizer A, Ulvestad A, Mills D, Dunning BE, Foley JE, Taskinen MR: Vildagliptin therapy reduces postprandial intestinal triglyceride-rich lipoprotein particles in patients with type 2 diabetes. Diabetologia. 2006;49:2049-2057

4. Taskinen MR, Bjornson E, Matikainen N, Soderlund S, Pietilainen KH, Ainola M, Hakkarainen A, Lundbom N, Fuchs J, Thorsell A, Andersson L, Adiels M, Packard CJ, Boren J: Effects of liraglutide on the metabolism of triglyceride-rich lipoproteins in type 2 diabetes. Diabetes Obes Metab. 2021;23:1191-1201

5. Matikainen N, Soderlund S, Bjornson E, Pietilainen K, Hakkarainen A, Lundbom N, Taskinen MR, Boren J: Liraglutide treatment improves postprandial lipid metabolism and cardiometabolic risk factors in humans with adequately controlled type 2 diabetes: A single-centre randomized controlled study. Diabetes Obes Metab. 2019;21:84-94

6. Whyte MB, Shojaee-Moradie F, Sharaf SE, Jackson NC, Fielding B, Hovorka R, Mendis J, Russell-Jones D, Umpleby AM: Lixisenatide Reduces Chylomicron Triacylglycerol by Increased Clearance. J Clin Endocrinol Metab. 2019;104:359-368

7. Hjerpsted JB, Flint A, Brooks A, Axelsen MB, Kvist T, Blundell J: Semaglutide improves postprandial glucose and lipid metabolism, and delays first-hour gastric emptying in subjects with obesity. Diabetes Obes Metab. 2018;20:610-619

8. Donnelly KL, Smith CI, Schwarzenberg SJ, Jessurun J, Boldt MD, Parks EJ: Sources of fatty acids stored in liver and secreted via lipoproteins in patients with nonalcoholic fatty liver disease. J Clin Invest. 2005;115:1343-1351

9. Armstrong MJ, Gaunt P, Aithal GP, Barton D, Hull D, Parker R, Hazlehurst JM, Guo K, team Lt, Abouda G, Aldersley MA, Stocken D, Gough SC, Tomlinson JW, Brown RM, Hubscher SG, Newsome PN: Liraglutide safety and efficacy in patients with non-alcoholic steatohepatitis (LEAN): a multicentre, double-blind, randomised, placebo-controlled phase 2 study. Lancet (London, England). 2016;387:679-690

10. Armstrong MJ, Hull D, Guo K, Barton D, Hazlehurst JM, Gathercole LL, Nasiri M, Yu J, Gough SC, Newsome PN, Tomlinson JW: Glucagon-like

peptide 1 decreases lipotoxicity in non-alcoholic steatohepatitis. J Hepatol. 2016;64:399-408
11. Gastaldelli A, Gaggini M, Daniele G, Ciociaro D, Cersosimo E, Tripathy D, Triplitt C, Fox P, Musi N, DeFronzo R, Iozzo P: Exenatide improves both hepatic and adipose tissue insulin resistance: A dynamic positron emission tomography study. Hepatology. 2016;64:2028-2037
12. Seghieri M, Rebelos E, Gastaldelli A, Astiarraga BD, Casolaro A, Barsotti E, Pocai A, Nauck M, Muscelli E, Ferrannini E: Direct effect of GLP-1 infusion on endogenous glucose production in humans. Diabetologia. 2013;56:156-161
13. Guerra S, Mocciaro G, Gastaldelli A: Adipose tissue insulin resistance and lipidome alterations as the characterizing factors of non-alcoholic steatohepatitis. Eur J Clin Invest. 2022;52:e13695
14. Masoodi M, Gastaldelli A, Hyotylainen T, Arretxe E, Alonso C, Gaggini M, Brosnan J, Anstee QM, Millet O, Ortiz P, Mato JM, Dufour JF, Oresic M: Metabolomics and lipidomics in NAFLD: biomarkers and non-invasive diagnostic tests. Nat Rev Gastroenterol Hepatol. 2021;18:835-856
15. Havulinna AS, Sysi-Aho M, Hilvo M, Kauhanen D, Hurme R, Ekroos K, Salomaa V, Laaksonen R: Circulating Ceramides Predict Cardiovascular Outcomes in the Population-Based FINRISK 2002 Cohort. Arterioscler Thromb Vasc Biol. 2016;36:2424-2430
16. Mantovani A, Dugo C: Ceramides and risk of major adverse cardiovascular events: A meta-analysis of longitudinal studies. J Clin Lipidol. 2020;14:176-185
17. Zobel EH, Wretlind A, Ripa RS, Rotbain Curovic V, von Scholten BJ, Suvitaival T, Hansen TW, Kjaer A, Legido-Quigley C, Rossing P: Ceramides and phospholipids are downregulated with liraglutide treatment: results from the LiraFlame randomized controlled trial. BMJ Open Diabetes Res Care. 2021;9
18. Jendle J, Hyotylainen T, Oresic M, Nystrom T: Pharmacometabolomic profiles in type 2 diabetic subjects treated with liraglutide or glimepiride. Cardiovasc Diabetol. 2021;20:237
19. Zhang L, Hu Y, An Y, Wang Q, Liu J, Wang G: The Changes of Lipidomic Profiles Reveal Therapeutic Effects of Exenatide in Patients With Type 2 Diabetes. Front Endocrinol. 2022;13:677202
20. Denimal D, Bergas V, Pais-de-Barros JP, Simoneau I, Demizieux L, Passilly-Degrace P, Bouillet B, Petit JM, Rouland A, Bataille A, Duvillard L, Verges B: Liraglutide reduces plasma dihydroceramide levels in patients with type 2 diabetes. Cardiovasc Diabetol. 2023;22:104
21. Camastra S, Astiarraga B, Tura A, Frascerra S, Ciociaro D, Mari A, Gastaldelli A, Ferrannini E: Effect of exenatide on postprandial glucose fluxes, lipolysis, and ss-cell function in non-diabetic, morbidly obese patients. Diabetes Obes Metab. 2017;19:412-420
22. Della Pepa G, Carli F, Sabatini S, Pezzica S, Russo M, Vitale M, Masulli M, Riccardi G, Rivellese AA, Vaccaro O, Bozzetto L, Gastaldelli A: Clusters of adipose tissue dysfunction in adults with type 2 diabetes identify those with worse lipidomic profile despite similar glycaemic control. Diabetes Metab Res Rev. 2024;40:e3798
23. Lemmens HJ, Bernstein DP, Brodsky JB: Estimating blood volume in obese and morbidly obese patients. Obes Surg. 2006;16:773-776
24. Sampson M, Ling C, Sun Q, Harb R, Ashmaig M, Warnick R, Sethi A, Fleming JK, Otvos JD, Meeusen JW, Delaney SR, Jaffe AS, Shamburek R, Amar M, Remaley AT: A New Equation for Calculation of Low-Density Lipoprotein Cholesterol in Patients With Normolipidemia and/or Hypertriglyceridemia. JAMA Cardiol. 2020;5:540-548
25. Mittendorfer B, Liem O, Patterson BW, Miles JM, Klein S: What does the measurement of whole-body fatty acid rate of appearance in plasma by using a fatty acid tracer really mean? Diabetes. 2003;52:1641-1648
26. Sanders FWB, Acharjee A, Walker C, Marney L, Roberts LD, Imamura F, Jenkins B, Case J, Ray S, Virtue S, Vidal-Puig A, Kuh D, Hardy R, Allison M, Forouhi N, Murray AJ, Wareham N, Vacca M, Koulman A, Griffin JL: Hepatic steatosis risk is partly driven by increased de novo lipogenesis following carbohydrate consumption. Genome Biol. 2018;19:79
27. Tschop M, Nogueiras R, Ahren B: Gut hormone-based pharmacology: novel formulations and future possibilities for metabolic disease therapy. Diabetologia. 2023;66:1796-1808
28. Watson E, Jonker DM, Jacobsen LV, Ingwersen SH: Population Pharmacokinetics of Liraglutide, a Once-Daily Human Glucagon-Like Peptide-1 Analog, in Healthy Volunteers and Subjects With Type 2 Diabetes, and Comparison to Twice-Daily Exenatide. The Journal of Clinical Pharmacology. 2013;50:886-894
29. Rhee EP, Cheng S, Larson MG, Walford GA, Lewis GD, McCabe E, Yang E, Farrell L, Fox CS, O'Donnell CJ, Carr SA, Vasan RS, Florez JC, Clish CB, Wang TJ, Gerszten RE: Lipid profiling identifies a triacylglycerol signature of insulin resistance and improves diabetes prediction in humans. J Clin Invest. 2011;121:1402-1411

30. Papandreou C, Harrold JA, Hansen TT, Halford JCG, Sjodin A, Bullo M: Changes in Circulating Metabolites during Weight Loss and Weight Loss Maintenance in Relation to Cardiometabolic Risk. Nutrients. 2021;13
31. Karpe F: Postprandial lipoprotein metabolism and atherosclerosis. J Intern Med. 1999;246:341-355
32. Mundra PA, Barlow CK, Nestel PJ, Barnes EH, Kirby A, Thompson P, Sullivan DR, Alshehry ZH, Mellett NA, Huynh K, Jayawardana KS, Giles C, McConville MJ, Zoungas S, Hillis GS, Chalmers J, Woodward M, Wong G, Kingwell BA, Simes J, Tonkin AM, Meikle PJ, Investigators LS: Large-scale plasma lipidomic profiling identifies lipids that predict cardiovascular events in secondary prevention. JCI Insight. 2018;3
33. Poss AM, Maschek JA, Cox JE, Hauner BJ, Hopkins PN, Hunt SC, Holland WL, Summers SA, Playdon MC: Machine learning reveals serum sphingolipids as cholesterol-independent biomarkers of coronary artery disease. J Clin Invest. 2020;130:1363-1376
34. Sigruener A, Kleber ME, Heimerl S, Liebisch G, Schmitz G, Maerz W: Glycerophospholipid and sphingolipid species and mortality: the Ludwigshafen Risk and Cardiovascular Health (LURIC) study. PLoS One. 2014;9:e85724
35. Luukkonen PK, Zhou Y, Sadevirta S, Leivonen M, Arola J, Oresic M, Hyotylainen T, Yki-Jarvinen H: Hepatic ceramides dissociate steatosis and insulin resistance in patients with non-alcoholic fatty liver disease. J Hepatol. 2016;64:1167-1175
36. Li Z, Lei H, Jiang H, Fan Y, Shi J, Li C, Chen F, Mi B, Ma M, Lin J, Ma L: Saturated fatty acid biomarkers and risk of cardiometabolic diseases: A meta-analysis of prospective studies. Front Nutr. 2022;9:963471
37. Varre JV, Holland WL, Summers SA: You aren't IMMUNE to the ceramides that accumulate in cardiometabolic disease. Biochim Biophys Acta Mol Cell Biol Lipids. 2022;1867:159125
38. Xiao C, Bandsma RH, Dash S, Szeto L, Lewis GF: Exenatide, a glucagon-like peptide-1 receptor agonist, acutely inhibits intestinal lipoprotein production in healthy humans. Arterioscler Thromb Vasc Biol. 2012;32:1513-1519
39. Schwartz EA, Koska J, Mullin MP, Syoufi I, Schwenke DC, Reaven PD: Exenatide suppresses postprandial elevations in lipids and lipoproteins in individuals with impaired glucose tolerance and recent onset type 2 diabetes mellitus. Atherosclerosis. 2010;212:217-222
40. Bunck MC, Corner A, Eliasson B, Heine RJ, Shaginian RM, Wu Y, Yan P, Smith U, Yki-Jarvinen H, Diamant M, Taskinen MR: One-year treatment with exenatide vs. insulin glargine: effects on postprandial glycemia, lipid profiles, and oxidative stress. Atherosclerosis. 2010;212:223-229
41. Dahl K, Brooks A, Almazedi F, Hoff ST, Boschini C, Baekdal TA: Oral semaglutide improves postprandial glucose and lipid metabolism, and delays gastric emptying, in subjects with type 2 diabetes. Diabetes Obes Metab. 2021;23:1594-1603
42. Stegemann C, Pechlaner R, Willeit P, Langley SR, Mangino M, Mayr U, Menni C, Moayyeri A, Santer P, Rungger G, Spector TD, Willeit J, Kiechl S, Mayr M: Lipidomics profiling and risk of cardiovascular disease in the prospective population-based Bruneck study. Circulation. 2014;129:1821-1831
43. Hodson L, Skeaff CM, Fielding BA: Fatty acid composition of adipose tissue and blood in humans and its use as a biomarker of dietary intake. Progress in lipid research. 2008;47:348-380
44. Wang Y, Meng X, Deng X, Okekunle AP, Wang P, Zhang Q, Ding L, Guo X, Lv M, Sun C, Li Y: Postprandial Saturated Fatty Acids Increase the Risk of Type 2 Diabetes: A Cohort Study in a Chinese Population. J Clin Endocrinol Metab. 2018;103:1438-1446
45. Cao C, Koh HE, Van Vliet S, Patterson BW, Reeds DN, Laforest R, Gropler RJ, Mittendorfer B: Increased plasma fatty acid clearance, not fatty acid concentration, is associated with muscle insulin resistance in people with obesity. Metabolism. 2022;132:155216
46. Vega RB, Whytock KL, Gassenhuber J, Goebel B, Tillner J, Agueusop I, Truax AD, Yu G, Carnero E, Kapoor N, Gardell S, Sparks LM, Smith SR: A Metabolomic Signature of Glucagon Action in Healthy Individuals With Overweight/Obesity. Journal of the Endocrine Society. 2021;5
47. Kalavalapalli S, Bril F, Guingab J, Vergara A, Garrett TJ, Sunny NE, Cusi K: Impact of exenatide on mitochondrial lipid metabolism in mice with nonalcoholic steatohepatitis. J Endocrinol. 2019;241:293-305
48. Liu P, Zhu W, Chen C, Yan B, Zhu L, Chen X, Peng C: The mechanisms of lysophosphatidylcholine in the development of diseases. Life Sci. 2020;247:117443
49. Kohno S, Keenan AL, Ntambi JM, Miyazaki M: Lipidomic insight into cardiovascular diseases. Biochem Biophys Res Commun. 2018;504:590-595
50. Hornburg D, Wu S, Moqri M, Zhou X, Contrepois K, Bararpour N, Traber GM, Su B, Metwally AA, Avina M, Zhou W, Ubellacker JM, Mishra T, Schussler-Fiorenza Rose SM, Kavathas PB, Williams KJ, Snyder MP: Dynamic lipidome alterations associated with human health, disease and ageing. Nat Metab. 2023;5:1578-1594.

SUPPLEMENTARY MATERIAL

Mixed Meal Tolerance Test Protocol

The mixed meal tolerance test (MTT) consisted of a standard meal (18% protein, 31% fat, and 51% carbohydrate, total caloric content 585 kcal) that was consumed within 10 min. Tracers ([$^{2}H_5$]glycerol and 6,6-[$^{2}H_2$]glucose) were infused as a primed-constant infusion starting 120 minutes before the meal and continued until the end of the study (360 min after meal ingetsion) for the measurement of lipolysis and glucose fluxes, i.e. glucose production and clearance (1). The MTT contained 1.5g of U^{13}C- glucose to measure glucose rate of absorption (1).

Arterialized blood samples were taken before the meal and then at regular intervals after the meal for 6 hours (i.e., 15, 30, 45, 60, 90, 120, 150, 180, 240, 300 and 360 min). Measurements of plasma apolipoprotein A and B concentration and lipidomic analyses were conducted on samples taken at 0, 180min and 360min considering that after mixed meals plasma TAG concentrations rise within 2-3 hours, reaching a plateau at 3-4 hours, and return to baseline by 6 hours (2).

Measurement of the lipidomic profile

Fasting plasma lipidomic profile was evaluated by liquid chromatography/quadrupole time-of-flight mass spectrometry (LC 1290 Infinity/MS Q-TOF -6545 Agilent Technology, Santa Clara, CA) equipped with an electrospray ionization source. Briefly, 10 µL of human plasma was deproteinized with 150 µL of cold methanol (Merck-Sigma-Aldrich, Darmstadt, Germany) and 10 µL of internal standard and centrifuged at 14000 rpm for 20 min. Subsequently, the supernatant was transferred into 0.2-mL glass inserts in screw-top vials with Teflon-lined caps (Agilent, Santa Clara, CA) and injected into the LC-MS QTOF. For liquid chromatography analysis, we used an Agilent ZORBAX Eclipse Plus C18 2.1 × 100 mm 1.8-Micron column at 50°C. Mobile phase A was water with 0.1% formic acid and mobile phase B was isopropanol/acetonitrile (1:1, v:v) with 0.1% formic acid. The injection volume was 1 µl and the untargeted acquisition was performed in positive mode.

The quantitative targeted analysis of the spectra (n=94) was performed with the Agilent MassHunter Profinder B.06.00, a mass spectrometry-based batch-targeted feature extraction software (Agilent, Santa Clara, CA). Lipid concentrations were calculated by relating the peak area of each lipid species to the peak area of the corresponding internal standard added to each sample before deproteinization within each lipid class; the internal standards were DAG(C34:0), TAG(C45:0), PC(C34:0), PE(C34:0), LPC(C17:0), SM(d18:1/17:0), CER(18:1/17:0) (Avanti Polar Lipids, Alabaster, AL and Larodan, Solna, SE). The proportion of unsaturated and saturated fat was evaluated using the number of double bonds for each lipid species and was considered as follows: 0-1 double bounds as saturated and ≥2 double bonds as unsaturated for DAG, PC and PE; 0-2 double bounds as saturated and ≥3 double bonds as unsaturated for TAG; 0 double bounds as saturated and ≥1 double bond as unsaturated for CER and LPC.

Plasma FFA composition was measured by gas chromatography-mass spectrometry (GC7890-MS5975, Agilent Technology, Santa Clara, CA) with electron ionization (EI). Briefly, 20 µL of plasma sample was mixed with heptadecanoic acid (C17:0) (Merck-Sigma-Aldrich, Darmstadt, Germany) as internal standard, 200 µL of methanol:chloroform 2:1, 100 µL of chloroform (Merck-Sigma-Aldrich, Darmstadt, Germany), and 100 µL of MilliQ water, vortexed and centrifuged at 14000 rpm for 20 min). The organic phase was dried under nitrogen flux, reconstituted with 80 µL of acetonitrile (Sigma-Aldrich), derivatized with 20 µL of N,O-Bis(trimethylsilyl)trifluoroacetamide with 1% trimethylchlorosilane (Merck-Sigma-Aldrich, Darmstadt, Germany) for 40 min at 75ºC and measured by GC-MS equipped with a capillary column (DB-5MS J&W, l 30 m; i.d. 0.25 mm; film thickness 0.25 µm, J&W, Agilent). FFA composition included myristic (C14:0), palmitoleic (C16:1), palmitic (C16:0), linoleic (C18:2), oleic (C18:1) and stearic (C18:0) acid. Retention times for each FFA were identified by a single injection of known standards (Merck-Sigma-Aldrich, Darmstadt, Germany). The percentage of each FFA was calculated as the area under the peak divided by the total area. Saturated FFA were calculated as the sum of myristic acid, palmitic acid, and stearic acid, and unsaturated FFA were calculated as the sum of palmitoleic acid, oleic acid, and linoleic acid.

Hormone measurements

Plasma insulin was measured by electro-chemiluminescence (COBASe411 instrument, Roche, Indianapolis, USA), and plasma glucagon by radioimmunoassay (Millipore Corporation, Billerica, MA, USA). Plasma GLP-1

and GIP concentrtaions were measured using a Milliplex® kit (Merck KGaA, Darmstadt, Germany) on Luminex® (Millipore Corporation, Billerica, MA, USA).

Fasting and postprandial insulin resistance measurements

Insulin resistance during fasting state was assessed as HOMA-IR, Hepatic-IR and Adipo-IR indexes, while in postprandial state $OGIS_{180}$ was used as index of peripheral insulin sensitivity, as previously reported (1; 3).

Tracer measurements and Calculations of lipid fluxes

Tracer enrichments were measured in plasma samples at all times by gas chromatography/mass spectrometry (GCMS *5975* Agilent Technologies, Fullerton, CA USA) as described previously (1).
Tracer data during fasting and postprandial state were analyzed with mathematical modeling for the quantification of rate of appearance of glycerol and glucose fluxes (i.e., glucose production, oral glucose rate of appearance during postprandial state and glucose clearance) as previously described (1; 3).
FFA uptake by peripheral tissues (Rd_FFA) was calculated as

$$Rd\_FFA(t)\ (umol/min) = Lipolysis(t)\ (umol/min) - dFFA(t)/dt \times Vol\ (ml/kg) \times BW\ (kg)$$

- Lipolysis(t) was estimated as 3 times Ra_glycerol(t), considering that during TAG hydrolysis 1 glycerol and 3 FFAs are released.
- $dFFA(t)/dt = [FFA(t)-FFA(t_1)]/(t-t_1)$; FFA(t) and $FFA(t_1)$ are the concentrations (umol/ml) measured at time t and at (t_1), i.e., the time point just before time (t);
- Vol is the volume of distribution that for FFA considered equal to plasma volume of distribution (4) and was estimated according to the formula proposed by Lemmens for subjects with severe obesity (5), i.e. Vol (ml/kg)=$70/\sqrt{(\mathrm{BMI}/22)}$.

References

1. Gastaldelli A: Measuring and estimating insulin resistance in clinical and research settings. Obesity. 2022;30:1549-1563
2. Lairon D, Lopez-Miranda J, Williams C: Methodology for studying postprandial lipid metabolism. Eur J Clin Nutr. 2007;61:1145-1161
3. Camastra S, Astiarraga B, Tura A, Frascerra S, Ciociaro D, Mari A, Gastaldelli A, Ferrannini E: Effect of exenatide on postprandial glucose fluxes, lipolysis, and ss-cell function in non-diabetic, morbidly obese patients. Diabetes Obes Metab. 2017;19:412-420
4. Romijn JA, Coyle EF, Sidossis LS, Gastaldelli A, Horowitz JF, Endert E, Wolfe RR: Regulation of endogenous fat and carbohydrate metabolism in relation to exercise intensity and duration. The American journal of physiology. 1993;265:E380-391
5. Lemmens HJ, Bernstein DP, Brodsky JB: Estimating blood volume in obese and morbidly obese patients. Obes Surg. 2006;16:773-776

Supplementary Table 1. Anthropometric, fasting, and postprandial parameters in the two treatment groups at the beginning and after 3 months of treatment.

	Control (n=15)		**Exenatide (n=15)**		***p*** [§]
	baseline	3 months	baseline	3 months	
Anthropometric parameters					
Gender (*n,* male/female)	3/12	-	1/14	-	0.999
Age (years)	46±7	-	47±8	-	0.946
Body weight (kg)	120±13	118±17	120±22	114±21*	**0.039**
BMI (kg/m^2)	45±3	44±5	45±8	43±6*	**0.043**
Waist circumference (cm)	131±9	128±13	127±12	119±9*	0.159
Fat-free mass (kg)	57±8	58±7	61±12	59±12	0.200
Fat mass (kg)	63±10	60±13*	60±11	55±12*	0.097
Glycemic control					
HbA1c (%)	5.8±0.3	5.8±0.3	5.8±0.4	5.7±0.4	0.078
HbA1c (mmol/L)	40±2	40±2	40±3	39±3	0.078
Fasting parameters					
HOMA-IR	4.6±2.3	4.4±2.2	5.1±2.5	4.3±2.2*	0.212
Glucose (mmol/L)	5.5±0.5	5.5±0.6	5.3±0.2	5.3±0.4	0.509
Insulin (pmol/L)	98±55	100±59	115±59	94±48*	0.054
GLP-1 (pg/ml)	146±254	137±240	72±84	61±38	0.268
GIP (pg/ml)	47±23	54±39	62±58	54±34	0.263
Glucagon (pmol/L)	26±15	26±14	23±7	24±7	0.970
Triglycerides (mg/dL)	93±34	92±35	99±32	97±40	0.904
Apo A1(mg/dL)	150±36	147±25	137±33	132±32	0.844
Apo B (mg/dL)	58±15	60±12	67±16	66±19	0.732
HDL Cholesterol (mg/dL)	52±11	49±11	44±10	41±9	0.660
LDL Cholesterol (mg/dL)	121±31	126±34	126±26	120±25	0.117
VLDL Cholesterol (mg/dL)	19±6	19±7	19±6	20±9	0.533
FFA (µM)	691±180	616±159	720±149	699±197	0.425
TAG [#] (µM)	636±171	611±134	650±182	611±172	0.800
DAG [#] (µM)	433±224	497±269	506±301	451±312	0.142
CER[#] (µM)	6±2	6±3	6±2	6±1	0.213
SM[#] (µM)	137±33	144±36	146±30	147±26	0.651
PC[#] (µM)	577±138	590±127	605±120	614±114	0.902
LPC[#] (µM)	156±21	156±26	168±21	160±19*	0.152
Postprandial parameters					
Glucose $AUC_{0\text{-}180}$ (mmol/l·min)	1302±157	1263±137	1225±124	1046±214*	**0.019**
Glucose $AUC_{180\text{-}360}$ (mmol/l·min)	977±105	951±203	980±97	993±141	0.605
Insulin $AUC_{0\text{-}180}$ (pmol/L·min)	96332±53564	89693±40792	102943±56977	58106±37475*	**0.038**
Insulin $AUC_{180\text{-}360}$ (pmol/L·min)	35971±24906	41064±31086	38116±18883	48061±32704	0.477
$OGIS_{0\text{-}180}$ (ml·min^{-1}·m^{-2})	316±42	308±52	310±39	359±43*	**0.002**
GLP-1 $AUC_{0\text{-}180}$ (pg/L·min)	38417±41569	37311±43057	20754±11139	13189±7825*	0.146
GLP-1 $AUC_{180\text{-}360}$ (pg/L·min)	34318±41699	29825±33000	16730±7599	15593±7985	0.383
GIP $AUC_{0\text{-}180}$ (pg/L·min)	55244±20635	54470±16887	62439±24979	37667±28052*	**0.017**
GIP $AUC_{180\text{-}360}$ (pg/L·min)	40688±17444	40653±14647	40626±14471	44027±19250	0.604
Glucagon $AUC_{0\text{-}180}$ (pmol/L·min)	4821±3453	4823±3107	4931±1694	3830±1086*	0.096
Glucagon $AUC_{180\text{-}360}$ (pmol/L·min)	5447±4341	5016±3430	4924±1630	3990±944	0.430

Data are presented as mean ± standard deviation. No differences at baseline between group, unpaired t-test. *p<0.05 vs baseline; [§]for between-treatments differences in variables changes (3 months *minus* baseline), ANCOVA general linear model. #sum of the concentrations of the single species. BMI: body mass index; HbA1c: glycated hemoglobin; HOMA-IR: homeostatic model assessment for insulin resistance; GLP-1: glucagon-like peptide 1; GIP: glucose-dependent insulinotropic polypepide; Apo: apolipoprotein; HDL: high density lipoprotein; LDL: low density lipoprotein; VLDL: very low-density lipoprotein; FFA: free fatty acid; TAG: triacylglycerols; DAG: diacylglycerols; CER: ceramides; SM: sphingomyelins; PC: phosphatidylcholines; LPC: lyso-phosphatidylcholines; OGIS: oral glucose insulin sensitivity; AUC: area under the curve.

Supplementary Table 2. Changes in single lipid species concentrations in the two treatment groups at the beginning and after 3 months of treatment.

		Control			Exenatide				Exenatide vs Control		
Lipid species (µM)	**Time**	**baseline**	**3 months *minus* baseline**	***p vs bas***	**baseline**	**3 months *minus* baseline**	***p vs bas***	***FDR adj***	***p EXE vs CT***	***FDR adj***	***p****
DAG(34:2)	0'	105.86±52.37	14.64±52.3	0.297	129.45±78.03	-31.24±70.03	0.106	0.366	0.051	0.221	0.167
	180'	49.91±32.69	3.84±32.85	0.669	54.16±45.78	-15.49±42.06	0.228	0.483	0.200	0.467	0.119
	360'	185.52±111.14	1.24±70.63	0.95	191.67±106.41	-18.34±137.85	0.64	0.806	0.652	0.789	0.899
DAG(34:1)	0'	116.88±53.97	14.5±32.95	0.111	133.32±74.41	-9.14±64.75	0.593	0.781	0.218	0.474	0.304
	180'	108.03±54.07	10.06±74.34	0.621	110.69±89.89	-26.54±83.87	0.296	0.539	0.249	0.527	0.166
	360'	181.25±100.84	16.68±58.6	0.325	182.8±128.67	-29.21±159.18	0.521	0.736	0.339	0.598	0.491
DAG(36:3)	0'	75.51±62.11	11.36±36.42	0.247	84.5±74.06	-0.78±45.26	0.948	0.964	0.425	0.651	0.396
	180'	37.13±34.08	6.01±24.71	0.379	41.57±35.03	-14.29±32.14	0.152	0.459	0.081	0.261	**0.025**
	360'	146.13±108.14	8.79±58.13	0.596	143.59±93.07	-4.15±113.9	0.898	0.944	0.718	0.826	0.813
DAG(36:2)	0'	134.55±66.87	23.93±45.25	0.06	158.62±94.44	-13.33±100.55	0.616	0.793	0.201	0.467	0.207
	180'	118.15±60.83	18.86±110.73	0.535	114.72±75.46	-21.35±74.86	0.344	0.594	0.297	0.568	0.103
	360'	196.27±127.43	28.29±62.05	0.126	198.32±113.14	-16.61±151.7	0.7	0.832	0.333	0.598	0.372
***sum* DAG**	0'	432.8±224.07	64.43±142.93	0.103	505.89±300.77	-54.49±269.08	0.446	0.692	0.141	0.382	0.212
	180'	313.22±172.97	38.77±236.19	0.55	321.14±243.26	-77.67±230.17	0.267	0.507	0.217	0.474	0.098
	360'	709.17±428.03	55±236.05	0.417	716.37±434.38	-68.3±558.5	0.667	0.827	0.470	0.675	0.605
TAG(44:1)	0'	1.99±0.81	0.44±1.33	0.219	2.71±2.25	-0.16±2.66	0.82	0.895	0.439	0.659	0.656
	180'	8.34±5.02	1.6±5.99	0.337	12.39±5.28	-8.66±6.95	**0.001**	**0.04**	**0.005**	**0.024**	**0.004**
	360'	4.48±3.17	0.18±2.19	0.775	4.63±2.69	-0.66±4.09	0.574	0.764	0.520	0.721	0.820
TAG(46:2)	0'	4.98±1.87	0.74±2.69	0.307	6.38±3.91	-1.22±3.94	0.249	0.494	0.122	0.355	0.696
	180'	11.68±5.62	2.13±6.64	0.251	16.05±6.06	-9.67±7.9	**0.001**	**0.04**	**0.000**	**0.022**	**0.004**
	360'	6.98±3.95	0.45±2.91	0.591	7.52±4.34	-1.18±5.87	0.482	0.712	0.379	0.629	0.815
TAG(46:1)	0'	6.12±2.28	1.12±3.59	0.249	6.78±3.48	-0.93±3.73	0.352	0.599	0.1379	0.376	0.594
	180'	14.58±7.12	2.09±7.78	0.334	19.44±7.65	-11.67±9.96	**0.002**	**0.040**	**0.000**	**0.025**	**0.007**
	360'	8.61±4.66	0.55±3.47	0.578	9.06±3.87	-2.13±5.67	0.201	0.473	0.159	0.408	0.433
TAG(46:0)	0'	2.96±1.23	0.25±1.8	0.594	3.25±1.98	-0.4±2	0.457	0.699	0.358	0.622	0.991

	180'	7.73±3.43	1.42±3.81	0.186	11.58±4.58	-7.71±5.51	**0.001**	**0.04**	**0.000**	**0.007**	**0.001**
	360'	5.91±3.39	0.05±2.62	0.945	5.76±3.04	-1.27±4.28	0.307	0.552	0.353	0.616	0.602
TAG(48:2)	0'	17.63±6.45	1.54±6.96	0.404	19.39±7.75	-2.7±8.1	0.217	0.476	0.134	0.371	0.551
	180'	32.59±14.18	2.62±16.21	0.555	37.93±12.95	-16.46±16.94	**0.006**	0.079	**0.007**	0.115	**0.024**
	360'	20.12±9.34	1.65±6.74	0.395	21.52±7.68	-4.62±11.89	0.187	0.473	0.111	0.341	0.396
TAG(48:1)	0'	19.01±7.22	-0.5±8.32	0.818	19.33±7.45	-2.39±7.72	0.251	0.494	0.526	0.721	0.796
	180'	34.05±14.25	2.58±14.89	0.528	39.89±12.79	-18.08±14.76	**0.001**	**0.04**	**0.001**	**0.049**	**0.019**
	360'	20.57±9.24	1±7.08	0.621	21.35±7.96	-4.48±11.93	0.201	0.473	0.167	0.417	0.466
TAG(48:0)	0'	8.03±3.67	-0.27±3.86	0.794	8.27±4.23	-1.34±3.92	0.208	0.476	0.457	0.67	0.955
	180'	15.63±6.43	1.03±5.77	0.516	20.32±7.44	-10.48±7.88	**0.001**	**0.04**	**0.001**	**0.019**	**0.003**
	360'	13.48±6.05	0.31±4.7	0.819	13.24±6.46	-3.1±8.52	0.215	0.476	0.219	0.474	0.471
TAG(50:4)	0'	6.15±3.54	-0.51±3.26	0.557	6.48±4.59	-0.71±3.41	0.435	0.684	0.870	0.933	0.892
	180'	8.15±3.65	-0.21±3.92	0.846	9.89±4.21	-4.53±3.62	**0.001**	**0.04**	**0.007**	0.117	**0.037**
	360'	6.25±3.94	-0.17±2.99	0.839	6.38±3.87	0.12±5.64	0.942	0.964	0.872	0.933	0.626
TAG(50:3)	0'	33.7±12.64	-0.45±8.76	0.845	35.62±13.37	-4.04±12.99	0.248	0.494	0.382	0.637	0.577
	180'	52.37±18.25	-0.25±17.32	0.958	56.62±15.06	-16.91±17.13	**0.006**	**0.079**	**0.021**	0.276	**0.027**
	360'	33.76±14.15	0.04±9.62	0.989	35.09±11.87	-4.02±19.21	0.465	0.705	0.502	0.702	0.905
TAG(50:2)	0'	57.32±16.58	-4.07±12.91	0.242	58.48±13.93	-6.3±16.39	0.159	0.459	0.683	0.801	0.847
	180'	85.52±25.35	1.05±24.21	0.873	89.03±20.24	-21.03±21.57	**0.006**	0.079	**0.022**	0.237	**0.017**
	360'	52.71±17.6	0.32±11.1	0.919	54.5±12.75	-7.06±20.67	0.241	0.494	0.267	0.546	0.577
TAG(50:1)	0'	51.34±16.35	-3.1±13.58	0.392	51.5±17.41	-5.9±17.25	0.207	0.476	0.625	0.789	0.846
	180'	83.2±26.35	1.44±23.05	0.819	88.98±23.71	-24.46±21.35	**0.002**	**0.044**	**0.006**	0.115	0.052
	360'	56.73±18.45	0.35±12.53	0.921	56.99±15.73	-7.38±21.69	0.243	0.494	0.276	0.549	0.571
TAG(50:0)	0'	3.62±1.88	0.05±1.91	0.916	4.1±3.16	-0.83±2.73	0.257	0.494	0.312	0.585	0.860
	180'	8.69±4.16	0.73±2.96	0.373	12.25±5.63	-7.01±5.77	**0.001**	**0.04**	**0.000**	**0.019**	**0.002**
	360'	7.54±5.1	-0.06±3.93	0.96	7.57±6.46	-1.98±7.76	0.375	0.625	0.432	0.657	0.668
TAG(52:5)	0'	9.58±5.49	-0.73±5.18	0.593	10.37±6.29	-0.8±4.19	0.472	0.708	0.968	0.968	0.993
	180'	12.14±5.89	-0.97±5.87	0.549	15.4±8.38	-6.55±7.07	**0.008**	0.085	**0.037**	0.203	**0.043**
	360'	9.48±6.44	-0.27±4.58	0.834	9.42±5.55	0.95±8.35	0.688	0.832	0.646	0.789	0.556
TAG(52:4)	0'	44.75±20.16	-0.88±15.86	0.833	46.43±19.29	-0.16±17.29	0.972	0.982	0.906	0.947	0.846

	180'	65.87±23.11	-1.43±18.39	0.776	76.7±23.44	-17.66±19.55	**0.01**	0.093	**0.039**	0.203	**0.029**
	360'	44.26±19.87	-0.55±13.67	0.888	46.2±16.77	3.69±22.21	0.56	0.76	0.563	0.741	0.545
TAG(52:3)	0'	100±30.36	-5.95±19.82	0.264	102.17±25.55	-2.17±28.81	0.774	0.861	0.679	0.799	0.748
	180'	141.62±34.49	1.08±27.53	0.885	152.57±29.46	-21.84±23.02	**0.007**	0.084	**0.031**	0.203	**0.025**
	360'	87.44±27.4	-0.42±17.22	0.932	92.12±19.7	-1.19±28.96	0.884	0.938	0.934	0.96	0.981
TAG(52:2)	0'	136.43±29.91	-5.48±31.67	0.513	132.64±28.65	-3.94±28.87	0.605	0.786	0.890	0.941	0.786
	180'	174.2±38.33	2.84±33.41	0.756	185.68±32.17	-22.7±26.06	**0.012**	0.103	**0.042**	0.210	0.065
	360'	114.1±25.38	2±16	0.66	117.26±17.23	-4.22±24.92	0.553	0.758	0.456	0.67	0.687
TAG(52:1)	0'	19.55±7.49	-1.2±5.94	0.447	19.8±11.18	-2.77±7.95	0.199	0.473	0.545	0.731	0.741
	180'	41.02±16.79	2.14±11.96	0.516	47.44±18.75	-19.32±16.48	**0.002**	**0.040**	**0.001**	**0.030**	**0.010**
	360'	25.24±15.41	-0.02±10.21	0.995	27.07±17.03	-5.55±21.13	0.362	0.607	0.403	0.645	0.753
TAG(52:0)	0'	1.47±0.62	-0.01±0.6	0.957	1.76±0.8	-0.16±0.98	0.535	0.743	0.610	0.776	0.586
	180'	3.12±1.35	0.56±0.83	0.025	4.22±1.64	-2.17±1.63	**0.001**	**0.04**	**0.001**	**0.003**	**0.001**
	360'	3.83±1.8	-0.12±1.36	0.748	3.34±2.31	-0.58±2.58	0.432	0.682	0.577	0.749	0.783
TAG(54:4)	0'	18.4±8.22	-1.61±6.21	0.333	18.2±7.39	1.31±5.88	0.401	0.656	0.196	0.467	0.552
	180'	24.03±9.08	1.39±9	0.574	32.07±9.62	-10.51±9.62	**0.003**	0.051	**0.003**	0.072	**0.001**
	360'	18.17±9.6	-0.28±5.78	0.865	19.46±4.75	1.28±6.68	0.502	0.725	0.530	0.723	0.986
TAG(54:3)	0'	54.15±16.47	-0.98±18.61	0.841	55.95±20.07	-1.55±16.83	0.727	0.832	0.931	0.960	0.658
	180'	83.39±22.44	2.51±16.86	0.587	94.09±23.4	-16.65±15.16	**0.003**	0.051	**0.005**	0.113	**0.005**
	360'	54.15±20.75	1.13±13	0.76	59.58±16.7	-2.07±21.23	0.731	0.832	0.647	0.789	0.539
TAG(54:2)	0'	27.82±7.84	-1.91±6.98	0.308	29.27±9.87	-1.22±8.38	0.583	0.774	0.808	0.892	0.733
	180'	53.09±13.84	1.45±9.66	0.584	56.67±14.29	-12.37±11.15	**0.003**	0.051	**0.002**	0.063	**0.009**
	360'	34.76±14.05	0.23±8.34	0.924	36.03±12.89	-2.5±18.46	0.634	0.802	0.631	0.789	0.783
TAG(54:1)	0'	3.46±1.18	-0.31±1.16	0.313	3.74±1.87	-0.34±1.4	0.356	0.599	0.946	0.965	0.293
	180'	9.89±3.38	0.37±2.61	0.605	9.58±4.52	-3.72±3.56	**0.004**	0.064	**0.002**	0.063	**0.028**
	360'	5.17±3.49	-0.31±2.33	0.638	5.2±3.51	-0.98±4.4	0.44	0.687	0.634	0.789	0.887
TAG(56:6)	0'	3.71±2.64	-0.62±2.32	0.322	2.92±1.55	0.23±1.19	0.471	0.708	0.221	0.474	0.469
	180'	4.26±3.02	-0.84±2.6	0.247	4.39±2.67	-1.7±2.68	0.050	0.253	0.415	0.645	0.394
	360'	4.21±3.21	-0.66±1.78	0.203	3.04±1.26	0.85±2.25	0.198	0.473	0.069	0.249	0.220
TAG(56:3)	0'	4±1.11	-0.27±1.21	0.396	4.24±1.73	-0.05±1.8	0.923	0.958	0.686	0.801	0.935

	180'	7.02±2.35	0.04±2.79	0.959	7.23±2.15	-1.37±1.97	**0.035**	0.215	0.157	0.407	0.064
	360'	5.03±2.87	-0.22±1.64	0.632	5.22±1.87	-0.09±3.34	0.921	0.958	0.901	0.946	0.902
***sum* TAG**	0'	636.19±171.41	-24.7±116.22	0.424	649.77±181.78	-38.52±174	0.406	0.658	0.889	0.887	0.934
	180'	982.18±263.1	25.37±228.08	0.684	1100.42±230.62	-293.22±207.78	**0.001**	**0.04**	**0.001**	**0.038**	**0.008**
	360'	642.98±223.37	5.16±143.98	0.899	667.56±177.96	-48.18±279.18	0.545	0.754	0.546	0.731	0.786
CER(d18:1/14:0)	0'	0.04±0.01	0±0.01	0.304	0.05±0.02	-0.01±0.01	**0.012**	**0.103**	**0.007**	0.115	**0.043**
	180'	0.03±0.01	0±0.01	0.754	0.04±0.01	0±0.01	0.81	0.89	0.966	0.968	0.402
	360'	0.04±0.01	0±0.02	0.372	0.04±0.02	-0.01±0.01	**0.039**	0.219	**0.036**	0.203	**0.047**
CER(d18:1/16:0)	0'	0.38±0.13	0.04±0.11	0.209	0.48±0.16	-0.03±0.12	0.354	0.599	0.122	0.355	0.155
	180'	0.32±0.09	0.02±0.09	0.318	0.35±0.12	0.04±0.1	0.17	0.468	0.637	0.789	0.782
	360'	0.48±0.17	0.07±0.19	0.206	0.48±0.18	-0.1±0.23	0.161	0.459	0.056	0.229	0.136
CER(d18:0/16:0)	0'	0.03±0.02	0±0.01	0.217	0.04±0.01	0±0.01	0.257	0.494	0.957	0.965	0.823
	180'	0.03±0.01	0±0.02	0.347	0.04±0.01	0±0.01	0.105	0.366	0.117	0.348	0.250
	360'	0.04±0.02	0.01±0.02	0.294	0.05±0.02	-0.01±0.02	0.098	0.362	0.054	0.225	0.085
CER(d18:1/18:1)	0'	0.05±0.02	0±0.02	0.625	0.06±0.02	0±0.02	0.402	0.656	0.335	0.598	0.269
	180'	0.04±0.01	0±0.01	0.599	0.04±0.01	0±0.01	0.263	0.503	0.638	0.789	0.894
	360'	0.06±0.02	0.01±0.03	0.348	0.06±0.03	-0.02±0.03	0.073	0.321	**0.046**	0.219	0.074
CER(d18:1/18:0)	0'	0.17±0.07	0.01±0.06	0.512	0.21±0.06	-0.01±0.06	0.552	0.758	0.371	0.626	0.306
	180'	0.16±0.05	0±0.05	0.736	0.17±0.04	0±0.03	0.729	0.832	0.932	0.96	0.857
	360'	0.23±0.09	0.03±0.13	0.368	0.24±0.1	-0.06±0.12	0.101	0.366	0.067	0.248	0.102
CER(d18:0/18:0)	0'	0.04±0.03	0±0.03	0.602	0.04±0.01	0±0.02	0.721	0.832	0.523	0.721	0.270
	180'	0.03±0.02	0±0.02	0.938	0.03±0.01	0±0.01	0.698	0.832	0.884	0.937	0.937
	360'	0.05±0.03	0.01±0.05	0.412	0.05±0.03	-0.02±0.03	**0.024**	0.176	0.066	0.248	**0.039**
CER(d18:1/20:0)	0'	0.17±0.06	0.02±0.05	0.148	0.23±0.07	-0.02±0.05	0.102	0.366	**0.027**	0.203	**0.042**
	180'	0.16±0.04	0±0.05	0.877	0.18±0.05	0±0.04	0.731	0.832	0.743	0.848	0.739
	360'	0.23±0.09	0.05±0.13	0.146	0.25±0.1	-0.06±0.14	0.149	0.459	**0.038**	0.203	**0.041**
CER(d18:0/20:0)	0'	0.02±0.01	0±0.01	0.305	0.03±0.01	0±0.01	0.692	0.832	0.288	0.566	0.387
	180'	0.02±0.01	0±0.01	0.18	0.03±0.01	0±0.01	0.82	0.895	0.479	0.681	0.728
	360'	0.02±0.01	0.01±0.03	0.17	0.02±0.01	-0.01±0.01	**0.036**	0.215	**0.048**	0.219	0.054

CER(d18:1/22:0)	0'	0.8±0.28	0.13±0.35	0.163	0.95±0.37	-0.09±0.23	0.158	0.459	**0.049**	0.219	**0.040**
	180'	0.89±0.26	0.14±0.43	0.257	0.93±0.23	0.03±0.27	0.708	0.832	0.470	0.675	0.883
	360'	1.06±0.35	0.36±0.61	0.056	1.1±0.45	-0.23±0.58	0.178	0.472	**0.018**	0.192	**0.023**
CER(d18:0/22:0)	0'	0.13±0.08	0.02±0.07	0.206	0.15±0.04	0±0.03	0.589	0.779	0.163	0.415	0.188
	180'	0.1±0.04	0.01±0.04	0.402	0.1±0.03	0±0.03	0.855	0.916	0.439	0.659	0.682
	360'	0.16±0.08	0.05±0.15	0.234	0.17±0.08	-0.05±0.09	0.060	0.287	**0.042**	0.210	**0.045**
CER(d18:1/24:1)	0'	1.4±0.56	0.15±0.6	0.339	1.56±0.54	0.05±0.45	0.675	0.83	0.594	0.765	0.451
	180'	1.49±0.55	0.14±0.55	0.353	1.54±0.46	0.07±0.36	0.505	0.725	0.717	0.826	0.806
	360'	1.85±0.74	0.43±0.79	0.076	1.89±0.72	-0.27±0.89	0.300	0.542	**0.046**	0.219	0.231
CER(d18:1/24:0)	0'	1.56±0.65	0.24±0.73	0.232	1.64±0.43	0.01±0.33	0.896	0.944	0.286	0.566	0.353
	180'	1.85±0.57	0.2±0.7	0.317	1.81±0.34	-0.01±0.38	0.926	0.958	0.374	0.626	0.979
	360'	2.63±0.89	0.53±1.07	0.097	2.47±0.87	-0.4±1.26	0.274	0.514	0.052	0.223	0.231
CER(d18:0/24:0)	0'	0.18±0.1	0.03±0.08	0.126	0.22±0.06	0±0.05	0.72	0.832	0.131	0.369	0.500
	180'	0.19±0.08	0.04±0.09	0.165	0.21±0.07	0.02±0.04	0.212	0.476	0.488	0.688	0.844
	360'	0.26±0.13	0.12±0.27	0.118	0.27±0.11	-0.07±0.13	0.08	0.341	**0.027**	0.203	**0.031**
CER(d18:1/25:0)	0'	0.47±0.15	0.09±0.23	0.142	0.58±0.25	0.06±0.15	0.163	0.459	0.610	0.776	0.987
	180'	0.55±0.16	0.1±0.27	0.203	0.59±0.23	0.09±0.13	**0.039**	0.219	0.928	0.96	0.702
	360'	0.69±0.22	0.24±0.39	0.047	0.72±0.24	-0.04±0.33	0.653	0.814	0.058	0.23	0.218
CER(d18:1/26:0)	0'	0.12±0.05	0.02±0.06	0.232	0.15±0.06	0.01±0.05	0.488	0.716	0.602	0.772	0.557
	180'	0.14±0.06	0.02±0.07	0.358	0.14±0.05	0.03±0.02	**0.001**	**0.04**	0.538	0.728	0.471
	360'	0.17±0.06	0.06±0.1	0.047	0.18±0.05	-0.01±0.07	0.523	0.736	**0.038**	0.203	**0.041**
CER(d18:0/26:0)	0'	0.03±0.02	0±0.02	0.65	0.03±0.01	0±0.01	0.557	0.759	0.873	0.933	0.915
	180'	0.03±0.02	0±0.01	0.393	0.04±0.02	0±0.01	0.997	0.997	0.548	0.731	0.776
	360'	0.03±0.01	0.01±0.02	0.213	0.04±0.01	-0.01±0.01	**0.024**	0.176	**0.021**	0.200	**0.033**
***sum* CER**	0'	5.59±2.05	0.78±2.11	0.175	6.43±1.82	-0.04±1.35	0.899	0.944	0.213	0.471	0.290
	180'	6.01±1.8	0.67±2.22	0.276	6.22±1.4	0.27±1.12	0.423	0.675	0.573	0.749	0.950
	360'	8±2.67	2±3.69	0.074	8.04±2.64	-1.36±3.8	0.223	0.477	**0.031**	0.203	0.121
***sum* dhCER**	0'	0.42±0.25	0.07±0.17	0.147	0.52±0.12	-0.01±0.12	0.829	0.899	0.173	0.427	0.310
	180'	0.4±0.17	0.06±0.17	0.228	0.45±0.13	0.01±0.08	0.601	0.782	0.411	0.645	0.989
	360'	0.55±0.27	0.21±0.52	0.166	0.6±0.23	-0.16±0.27	0.055	0.271	**0.030**	0.203	**0.043**

PC aa(30:0)	0'	1.92±1.19	0.27±1.54	0.509	2.14±0.88	-0.14±0.92	0.574	0.765	0.388	0.633	0.997
	180'	2±1.36	-0.16±1.26	0.639	1.85±0.7	-0.38±1.05	0.24	0.494	0.643	0.789	0.395
	360'	2.15±1.43	0.45±1.41	0.277	2.05±1.06	-0.64±1.37	0.121	0.399	0.059	0.231	0.208
PC aa(32:2)	0'	1.37±0.69	0.12±0.99	0.639	1.49±0.72	-0.16±0.49	0.228	0.483	0.332	0.598	0.961
	180'	1.42±0.74	0.07±1.04	0.809	1.32±0.4	-0.14±0.71	0.503	0.725	0.558	0.739	0.573
	360'	1.31±0.64	0.32±0.73	0.146	1.3±0.67	-0.29±0.88	0.255	0.494	0.067	0.248	0.302
PC aa(32:1)	0'	13.27±6.53	0.75±6.96	0.681	14.04±6.29	-3.23±4.79	**0.021**	0.167	0.078	0.263	0.271
	180'	14.07±8.02	-1.28±6.28	0.458	12.06±4.75	-2.41±5.87	0.183	0.473	0.643	0.789	0.555
	360'	13.19±7.11	1.54±6.26	0.393	12.25±4.87	-3.62±6.32	0.061	0.288	**0.047**	0.219	**0.043**
PC aa(32:0)	0'	7.65±2.49	0.72±2.76	0.33	8.54±2.61	-0.12±2.22	0.836	0.899	0.366	0.625	0.509
	180'	8.28±2.59	0.05±2.86	0.947	7.91±1.6	0.24±1.77	0.654	0.814	0.848	0.923	0.508
	360'	8.07±2.81	0.91±3.29	0.338	7.96±2.78	-1.46±3.3	0.137	0.438	0.079	0.261	0.138
PC(16:0/18:2)	0'	3.13±1.06	0.36±1.12	0.239	3.06±1.41	0.2±0.83	0.377	0.625	0.659	0.795	0.988
	180'	3.29±1.17	0.34±1.76	0.477	3.16±1.16	-0.3±1.32	0.447	0.692	0.308	0.582	0.363
	360'	3.11±1.25	0.71±1.33	0.08	2.91±1.62	-0.51±1.33	0.19	0.473	**0.028**	0.203	0.061
PC aa(34:4)	0'	0.2±0.15	-0.02±0.15	0.667	0.16±0.08	0.03±0.07	0.125	0.406	0.269	0.546	0.099
	180'	0.14±0.07	-0.01±0.08	0.642	0.15±0.07	-0.05±0.09	0.086	0.347	0.293	0.567	0.784
	360'	0.2±0.14	0.02±0.1	0.519	0.17±0.1	0±0.15	0.93	0.958	0.673	0.798	0.739
PC aa(34:3)	0'	1.22±0.48	0.07±0.44	0.547	1.21±0.54	0.03±0.49	0.802	0.885	0.822	0.903	0.922
	180'	1.31±0.76	0.09±1.05	0.759	1.12±0.33	-0.06±0.56	0.712	0.832	0.663	0.795	0.918
	360'	1.12±0.39	0.05±0.35	0.619	1.1±0.46	-0.13±0.56	0.415	0.67	0.333	0.598	0.557
PC aa(34:2)	0'	175.35±40.47	7.39±44.46	0.53	182.26±47.77	1.84±25.26	0.783	0.866	0.677	0.799	0.736
	180'	149.07±23.53	11.86±34.38	0.219	155.49±19.2	-8.77±19.87	0.155	0.459	0.079	0.26	0.177
	360'	192.5±42.29	17.2±45.56	0.199	205.94±60.92	-31.84±66.81	0.111	0.38	0.038	0.203	0.057
PC aa(34:1)	0'	122.76±27.61	4.17±25.67	0.539	134.22±31.06	-5.64±22.33	0.344	0.594	0.273	0.547	0.548
	180'	119.88±31.14	4.47±30.1	0.587	122.36±21.62	-4.12±20.38	0.499	0.725	0.410	0.645	0.608
	360'	147.01±39.47	7.71±26.38	0.313	151.5±40.2	-22.59±47.94	0.115	0.388	0.057	0.229	0.100
PC(16:0/20:4)	0'	2.01±1.12	-0.22±0.9	0.355	1.62±0.7	0.47±0.69	**0.020**	0.167	0.025	0.203	**0.031**
	180'	1.64±0.8	-0.03±0.94	0.897	1.68±0.73	-0.32±0.9	0.241	0.494	0.433	0.657	0.231
	360'	2.48±1.45	0±0.94	0.994	2.11±1.06	0.15±1.01	0.598	0.782	0.691	0.803	0.634

PC(18:0/18:3)	0'	2.86±1.59	-0.19±1.22	0.557	2.6±1.18	0.92±1.54	**0.036**	0.215	**0.036**	0.203	0.094
	180'	2.81±1.47	-0.08±1.37	0.838	3.04±1.52	-0.66±1.68	0.205	0.473	0.338	0.598	0.235
	360'	3.55±2.17	0.35±1.67	0.458	3.04±1.38	0.27±2.34	0.683	0.832	0.917	0.956	0.869
PC aa(36:5)	0'	1.77±2.23	-0.35±2.39	0.576	0.94±0.72	0.28±0.61	0.096	0.361	0.328	0.598	0.465
	180'	1.45±1.6	-0.48±1.52	0.255	1.34±1.49	-0.74±1.38	0.091	0.351	0.664	0.795	0.744
	360'	1.87±1.86	-0.14±2.03	0.807	1.15±0.88	0±1.14	0.988	0.991	0.835	0.912	0.855
PC aa(36:4)	0'	26.75±13.78	-3.53±9.35	0.165	21.9±8.23	7.12±8.57	**0.006**	0.079	**0.003**	0.069	**0.013**
	180'	20.72±8.79	-1.12±9.62	0.67	23.64±8.12	-4.47±11.42	0.202	0.473	0.424	0.651	0.322
	360'	35.68±16.7	-2.43±8.75	0.336	33.67±13.19	1.04±17.77	0.836	0.899	0.532	0.723	0.576
PC aa(36:3)	0'	52.58±16.58	-0.05±14.58	0.99	52.34±17	4.11±12.2	0.213	0.476	0.404	0.645	0.317
	180'	51.46±15.39	0.83±19.17	0.874	56.56±12.94	-10.42±21.19	0.116	0.388	0.167	0.417	0.243
	360'	70.47±26.49	5.11±20.71	0.391	69.36±28.6	-10.94±39.49	0.338	0.593	0.206	0.467	0.370
PC aa(36:2)	0'	93.73±26.1	6.32±26.25	0.367	107.55±19.12	0.86±15.85	0.836	0.899	0.496	0.695	0.868
	180'	97.03±26.86	10.03±27.64	0.197	115.62±16.75	-14.09±23.84	0.065	0.296	**0.026**	0.203	**0.039**
	360'	115.03±30.59	15.52±33.49	0.121	137.7±42.48	-27.13±47.06	0.06	0.287	**0.013**	0.157	**0.045**
PC aa(36:1)	0'	28.29±10.66	3.32±8.92	0.172	33.01±9.18	-2.66±9.03	0.273	0.514	0.079	0.266	0.348
	180'	37.2±16.79	0.18±14.52	0.964	38.54±11.11	-5.35±16.58	0.287	0.529	0.373	0.626	0.902
	360'	39.82±18.28	4.9±14.81	0.256	41.79±18.12	-10.59±26.44	0.174	0.471	0.077	0.260	0.236
PC aa(38:6)	0'	6.46±5.85	-1.72±4.64	0.173	3.61±2.87	2.33±3.65	**0.027**	0.187	**0.012**	0.154	**0.016**
	180'	5.84±4.77	-1.25±3.96	0.259	6.73±7.12	-3.1±7.4	0.174	0.471	0.424	0.651	0.349
	360'	8.62±7.58	-1.23±5.2	0.409	5.78±5.32	0.61±5.68	0.707	0.832	0.397	0.644	0.703
PC aa(38:5)	0'	2.73±1.54	-0.29±1.21	0.364	2.2±1.01	0.72±0.95	**0.011**	0.102	**0.016**	0.177	**0.028**
	180'	2.01±1.05	-0.07±1.27	0.838	2.54±1.84	-0.79±1.87	0.168	0.467	0.252	0.527	0.185
	360'	3.66±2.33	-0.34±1.22	0.334	3.31±1.31	0.28±1.73	0.563	0.76	0.296	0.568	0.450
PC aa(38:4)	0'	13.63±6.89	-1.45±4.7	0.252	13.06±4.54	2.4±4.02	**0.036**	0.215	**0.022**	0.200	**0.036**
	180'	12.52±5.73	-0.15±5.85	0.923	16.79±7.59	-4.34±8.08	0.09	0.351	0.139	0.378	0.174
	360'	18.1±8.79	-0.6±5.32	0.693	19.47±7.22	-0.77±8.36	0.744	0.838	0.949	0.965	0.764
PC aa(38:3)	0'	15.74±7.77	-1.23±5.75	0.422	16.63±8.35	-1.33±4.64	0.285	0.527	0.956	0.965	0.639
	180'	17.41±7.35	-0.61±7.87	0.775	21.83±9.63	-7.63±10.65	**0.03**	0.203	0.065	0.248	0.176
	360'	21.06±11.65	0.82±8.91	0.746	23.53±15.71	-8.27±18.94	0.142	0.447	0.130	0.369	0.337

PC aa(40:6)	0'	2.51±2.14	-0.67±1.73	0.154	1.72±1.25	0.66±1.14	**0.042**	0.220	**0.019**	0.190	**0.040**
	180'	2.32±1.72	-0.47±1.38	0.229	3.21±3.55	-1.78±3.47	0.103	0.366	0.203	0.467	0.238
	360'	3.47±2.88	-0.52±1.97	0.355	2.71±2.25	-0.04±2.42	0.959	0.972	0.576	0.749	0.654
PC aa(40:5)	0'	0.41±0.31	-0.07±0.29	0.374	0.35±0.21	0.03±0.15	0.514	0.735	0.271	0.546	0.343
	180'	0.33±0.21	-0.03±0.22	0.624	0.47±0.48	-0.25±0.46	0.084	0.347	0.121	0.355	0.143
	360'	0.54±0.44	-0.06±0.33	0.531	0.51±0.29	-0.04±0.37	0.729	0.832	0.873	0.933	0.739
PC aa(40:4)	0'	0.36±0.22	-0.04±0.17	0.386	0.33±0.18	-0.02±0.11	0.475	0.71	0.721	0.826	0.557
	180'	0.35±0.18	0±0.23	0.995	0.44±0.23	-0.2±0.22	**0.009**	0.087	**0.033**	0.203	**0.045**
	360'	0.42±0.31	-0.03±0.25	0.71	0.44±0.3	-0.14±0.36	0.194	0.473	0.366	0.625	0.632
***sum* PC**	0'	576.72±137.98	13.66±128.64	0.687	605.01±120.42	8.69±86.78	0.704	0.832	0.902	0.946	0.623
	180'	552.55±131.19	22.17±136.34	0.553	597.85±79.07	-70.14±121.22	0.07	0.315	0.082	0.261	0.210
	360'	693.41±187.27	50.24±166.8	0.299	729.76±206.43	-116.63±276.97	0.155	0.459	0.075	0.259	0.169
LPC(14:0)	0'	0.61±0.22	0.05±0.35	0.551	0.67±0.19	-0.1±0.2	0.081	0.341	0.154	0.403	0.937
	180'	0.73±0.33	0±0.36	0.993	0.72±0.16	-0.16±0.23	**0.039**	0.219	0.212	0.471	0.896
	360'	0.76±0.35	0.09±0.29	0.31	0.71±0.17	-0.12±0.24	0.105	0.366	0.065	0.248	0.429
LPC(16:1)	0'	1.71±0.36	0±0.37	0.989	1.87±0.35	-0.25±0.31	**0.007**	0.084	0.054	0.225	0.281
	180'	2.06±0.49	-0.05±0.52	0.73	2.05±0.35	-0.34±0.37	**0.008**	0.085	0.115	0.346	0.360
	360'	2.33±0.46	0.03±0.36	0.8	2.23±0.35	-0.22±0.55	0.181	0.472	0.194	0.467	0.557
LPC(16:0)	0'	62.91±9	-1.1±8.85	0.638	63.74±12.44	-3.09±4.87	0.028	0.188	0.451	0.669	0.964
	180'	58.67±5.78	3.62±15.24	0.39	61.01±6	-2.53±6.45	0.201	0.473	0.205	0.467	0.196
	360'	84.28±9.16	-1.11±4.25	0.364	85.9±10.16	-7.25±14.14	0.089	0.351	0.147	0.391	0.111
LPC(18:2)	0'	19.4±4.17	1.35±6.33	0.421	20.95±3.92	0.79±4.05	0.463	0.705	0.773	0.866	0.552
	180'	16.8±4.72	1.97±4.03	0.091	18.82±3.9	-2.94±4.92	0.062	0.288	**0.010**	0.136	**0.017**
	360'	25.07±4.37	1.97±3.79	0.086	26.97±5.5	-1.72±4.69	0.210	0.476	**0.037**	0.203	**0.042**
LPC(18:1)	0'	21.39±4.31	1.11±3	0.175	23.9±3.12	-0.97±2.51	0.157	0.459	**0.049**	0.219	**0.031**
	180'	21.6±4.86	1.33±4.6	0.298	23.72±3.39	-1.78±2.1	**0.014**	0.116	**0.041**	0.21	**0.039**
	360'	28.37±4.9	1.08±2.91	0.205	29.08±4.45	-2.16±5.47	0.18	0.472	0.071	0.249	0.112
LPC(18:0)	0'	41.53±9.58	1.27±7.49	0.524	49.34±8.41	-5.43±5.48	**0.002**	**0.04**	**0.009**	0.132	**0.001**
	180'	47.73±7.9	2.31±9.74	0.39	53.99±6.47	-5.03±7.5	**0.04**	0.22	**0.044**	0.213	**0.036**

	360'	58.57±8.05	1.74±8.34	0.467	63.23±10.46	-10.03±11.36	**0.008**	0.085	**0.006**	0.113	**0.004**
LPC(20:4)	0'	4.45±1.78	-0.5±1.54	0.228	4.26±1.33	0.57±0.94	**0.034**	0.215	**0.029**	0.203	**0.027**
	180'	3.43±1.33	0.08±1.36	0.835	3.88±1.51	-0.42±1.44	0.335	0.592	0.375	0.626	0.334
	360'	6.43±2.51	-0.7±1.19	0.057	6.15±2.11	0.08±1.76	0.866	0.925	0.198	0.467	0.160
LPC(20:3)	0'	3.07±0.85	-0.35±0.82	0.122	3.29±1.2	-0.3±0.76	0.149	0.459	0.867	0.933	0.497
	180'	2.2±0.76	-0.04±0.8	0.855	2.63±0.94	-0.65±0.92	**0.032**	0.208	0.082	0.261	0.080
	360'	4.24±1.44	-0.17±0.87	0.503	4.46±1.55	-0.77±1.25	**0.047**	0.242	0.168	0.417	0.365
LPC(22:6)	0'	0.79±0.45	-0.14±0.34	0.137	0.7±0.2	0.13±0.27	0.092	0.351	**0.025**	0.203	**0.029**
	180'	0.61±0.31	-0.02±0.21	0.716	0.75±0.49	-0.13±0.45	0.327	0.583	0.407	0.645	0.302
	360'	1.15±0.62	-0.14±0.45	0.298	1.03±0.33	0.04±0.31	0.672	0.83	0.265	0.546	0.629
***sum* LPC**	0'	155.86±21.25	1.7±23.84	0.786	168.73±21.07	-8.65±13.2	**0.024**	0.176	0.152	0.401	0.732
	180'	153.83±17.69	9.2±27.83	0.238	167.57±12.1	-13.99±11.35	**0.001**	**0.04**	**0.012**	0.154	**0.032**
	360'	211.19±14.3	2.79±13.74	0.478	219.76±19.39	-22.14±30.12	**0.021**	0.167	**0.012**	0.154	**0.047**
PE(34:2)	0'	6.39±1.79	0.58±4.29	0.608	6.29±2.92	0.37±3.03	0.642	0.806	0.877	0.934	0.896
	180'	7.67±3.88	-1.76±3.95	0.118	5.19±3.45	-0.43±4.82	0.762	0.852	0.446	0.666	0.376
	360'	4.78±0.88	0.19±2.17	0.756	4.79±1.9	-0.92±2.04	0.131	0.422	0.192	0.465	0.339
PE(36:2)	0'	2.94±1.22	0.3±1.61	0.481	3.07±1.14	0.61±1.26	0.081	0.341	0.559	0.739	0.190
	180'	4.45±1.57	0.48±2.35	0.459	5.39±1.92	-1.06±2.69	0.202	0.473	0.133	0.371	0.385
	360'	2.1±0.86	0.29±1.03	0.324	2.11±1.3	-0.24±1.67	0.611	0.791	0.335	0.598	0.764
PE(38:4)	0'	0.51±0.32	-0.04±0.29	0.562	0.38±0.16	0.21±0.24	**0.005**	0.072	**0.014**	0.163	**0.015**
	180'	0.56±0.24	0±0.32	0.981	0.71±0.45	-0.21±0.51	0.176	0.472	0.206	0.467	0.356
	360'	0.45±0.28	-0.04±0.18	0.407	0.35±0.18	0.05±0.35	0.635	0.801	0.412	0.645	0.260
PE(38:3)	0'	1.34±0.28	-0.1±0.4	0.352	1.29±0.28	0.11±0.33	0.216	0.476	0.128	0.368	**0.035**
	180'	1.45±0.38	0.06±0.45	0.642	1.8±0.59	-0.43±0.68	0.051	0.253	0.038	0.203	0.102
	360'	0.91±0.26	0.02±0.26	0.817	1±0.36	-0.12±0.43	0.342	0.594	0.343	0.603	0.506
PE(38:2)	0'	7.91±2.94	0.86±3.28	0.327	8.7±2.92	1.99±3.42	**0.041**	0.22	0.364	0.625	0.165
	180'	14.82±6.94	0.83±7.21	0.672	17.81±5.86	-2.77±8.48	0.282	0.526	0.253	0.527	0.420
	360'	6.51±3.2	0.97±3.1	0.28	6.53±3.69	-0.49±5.13	0.734	0.832	0.385	0.633	0.664
PE(38:1)	0'	6.97±2.61	0.23±1.67	0.597	6.93±2.13	0.87±1.87	0.092	0.351	0.333	0.598	0.233
	180'	12.91±6.13	-1.17±4.75	0.376	12.71±3.28	-1.27±4.36	0.335	0.592	0.954	0.965	0.739

	360'	5.01±3.05	0.51±2.55	0.484	4.43±2.18	-0.47±3.38	0.628	0.801	0.413	0.645	0.601
***sum* PE**	0'	26.05±6.49	1.83±8.57	0.422	26.67±6.76	4.16±8.64	0.083	0.347	0.464	0.673	0.267
	180'	41.86±15.15	-1.56±14.65	0.697	43.61±12.37	-6.17±17.71	0.253	0.494	0.474	0.677	0.782
	360'	19.76±7.03	1.94±7.58	0.374	19.21±8.49	-2.19±12.13	0.528	0.736	0.308	0.582	0.567
SM(d16:1/18:1) or SM(d18:2/16:0)	0'	14.84±3.94	1.02±3.92	0.33	16.11±4.26	-0.02±3.7	0.985	0.991	0.461	0.672	0.680
	180'	17.15±4.43	0.45±5.96	0.781	16.94±4.04	-0.32±3.38	0.746	0.838	0.693	0.803	0.778
	360'	15.89±3.59	1.78±4.48	0.178	15.7±5.13	-2.16±6.04	0.222	0.477	0.071	0.249	0.182
SM(d18:0/16:0)	0'	3.75±1.13	0.71±1.2	0.038	4.55±1.1	0.27±0.94	0.293	0.537	0.269	0.546	0.335
	180'	4.06±1.1	0.51±1.03	0.088	4.35±0.76	0.4±0.54	**0.025**	0.18	0.755	0.855	0.988
	360'	4.27±1.21	0.9±1.54	0.057	4.61±1.37	-0.58±1.68	0.241	0.494	**0.028**	0.203	0.067
SM(d16:1/22:0)	0'	13.38±3.19	1.03±2.83	0.179	14.75±2.93	-1±2.62	0.164	0.459	0.051	0.221	0.208
	180'	15.44±2.54	0.44±4.2	0.704	15.3±2.47	-0.45±2.39	0.528	0.736	0.524	0.721	0.997
	360'	16.06±4.32	2.42±5.6	0.146	15.33±4.15	-2.23±5.24	0.151	0.459	**0.039**	0.203	0.166
SM(d18:2/22:1)	0'	1.37±0.33	-0.06±0.31	0.436	1.45±0.37	0.05±0.47	0.708	0.832	0.452	0.669	0.784
	180'	1.43±0.27	-0.02±0.26	0.774	1.36±0.29	0.03±0.35	0.735	0.832	0.647	0.789	0.731
	360'	1.76±0.42	0.08±0.45	0.518	1.72±0.5	-0.13±0.59	0.453	0.698	0.318	0.593	0.228
SM(d16:1/24:1) or SM (d18:1/22:1) or SM(d18:2/22:0)	0'	19.28±4.17	0.85±4.09	0.433	20.03±4.03	-0.77±4.2	0.489	0.716	0.293	0.567	0.488
	180'	23.11±4.13	0.16±6.4	0.925	21.51±3.19	-0.72±3.43	0.48	0.712	0.671	0.798	0.942
	360'	21.91±5.1	2.52±6.61	0.194	20.7±5.76	-2.57±7.1	0.216	0.476	0.070	0.249	0.255
SM(d16:1/24:0)	0'	18.27±5.74	1.23±4.55	0.312	19.35±4.3	-1.28±3.88	0.222	0.477	0.114	0.346	0.395
	180'	23.88±4.84	0.44±8.52	0.851	22.29±3.18	-0.33±3.9	0.775	0.861	0.777	0.867	0.683
	360'	20.21±6.94	3.53±7.26	0.105	18.98±6.18	-3.11±8.07	0.19	0.473	**0.037**	0.203	0.176
SM(d17:1/24:1) or SM(d18:2/23:0)	0'	7.77±1.97	0.27±1.92	0.592	8.1±1.87	0.04±2.13	0.941	0.964	0.758	0.855	0.784
	180'	10.02±1.92	0.19±3.27	0.832	9.4±1.82	-0.04±1.9	0.946	0.964	0.833	0.912	0.999
	360'	8.47±2.26	1.19±2.83	0.156	8.03±2.37	-0.79±3.25	0.401	0.656	0.111	0.341	0.222
SM(d18:2/24:1)	0'	21.48±5.54	0.52±4.54	0.665	23.01±5.88	1.22±7.1	0.518	0.736	0.750	0.853	0.860

	180'	26.52±5.39	-0.04±6.85	0.982	25.24±6.38	0.6±5.72	0.725	0.832	0.800	0.887	0.662
	360'	25.06±6.04	2.67±7.26	0.21	24.3±8.31	-1.46±8.96	0.567	0.763	0.208	0.468	0.188
SM(d18:2/24:0)	0'	36.95±10.99	1.72±9.85	0.51	38.42±8.94	3.11±14.61	0.423	0.675	0.761	0.856	0.870
	180'	49.19±11.04	0.05±15.58	0.99	44.43±8.28	3.86±11.03	0.251	0.494	0.486	0.688	0.863
	360'	42.61±12.61	6.42±14.58	0.138	39.84±13.88	-2.62±19.06	0.629	0.801	0.186	0.455	0.177
***sum* SM**	0'	137.09±33.24	7.29±30.23	0.366	145.76±29.89	1.62±37.4	0.87	0.925	0.651	0.789	0.647
	180'	170.8±31.9	2.18±48.95	0.87	160.84±24.57	3.02±27.14	0.707	0.832	0.958	0.965	0.992
	360'	156.23±39.07	21.51±47.47	0.128	149.2±43.94	-15.63±57.69	0.348	0.596	0.085	0.268	0.166

False Discovery Rate (FDR) was calculated for changes in EXE vs baseline and EXE vs CT (not shown for CT vs baseline as none of the changes were significant).
*p value adjusted for changes in body weight (3 months *minus* baseline). DAG: diacylglycerol; CER: ceramide; dhCER: dihydroceramide; PC: phosphatidylcholine; LPC: lysophosphatidylcholine; PE: phosphatidylethanolamine; SM: sphingomyelin; TAG: triacylglycerol.

Supplementary Table 3. Correlation analyses between changes in the most significative metabolic changes.

	R value	*p*	*p* adj*
$\Delta AUC_{0\text{-}180\ min}$ Clearance FFA vs			
HOMA-IR	**0.48**	**0.008**	**0.05**
AT-IR	0.09	0.65	0.37
Hepatic-IR	0.03	0.90	0.17
OGIS	**-0.58**	**0.0009**	**0.002**
$\Delta AUC_{0\text{-}180\ min}$ Glucose	**0.57**	**0.001**	**0.008**
$\Delta AUC_{0\text{-}180\ min}$ Insulin	**0.61**	**0.0005**	**0.003**
$\Delta AUC_{0\text{-}180\ min}$ TG	0.18	0.35	0.773
$\Delta Palmitate_{180\ min}$ vs			
HOMA-IR	-0.38	0.04	0.119
AT-IR	-0.09	0.65	0.093
Hepatic-IR	0.02	0.91	0.51
OGIS	**0.71**	**0.00001**	**0.002**
$\Delta AUC_{0\text{-}180\ min}$ Glucose	**-0.66**	**0.00001**	**0.00002**
$\Delta AUC_{0\text{-}180\ min}$ Insulin	**-0.46**	**0.01**	**0.02**
$\Delta AUC_{0\text{-}180\ min}$ TG	-0.18	0.35	0.76